On the dynamical downscaling and bias correction of seasonal-scale winter precipitation predictions over North India

P.R. Tiwari[1], S.C. Kar[2*], U.C. Mohanty[3], S. Dey[1], P. Sinha[4], P.V.S. Raju[5] and M.S. Shekhar[6]

[1]Centre for Atmospheric Sciences, IIT Delhi, India

[2]National Centre for Medium Range Weather Forecasting, Noida, India

[3]School of Earth Ocean and Climate Sciences, IIT Bhubaneswar, India

[4]Department of Meteorology, Pennsylvania State University, USA

[5] Center of Excellence for Climate Change Research, King Abdulaziz University, Saudi Arabia

[6]Snow and Avalanche Study Establishment, Chandigarh, India

*Correspondence
Dr. S.C. Kar
National Centre for Medium Range Weather Forecasting (NCMRWF),
A-50, Sector-62, Noida, India
Email: sckar@ncmrwf.gov.in

Abstract

This study presents the results of high-resolution (30 km) climate simulations over North India using an optimized configuration of the Regional Climate Model (RegCM), driven by a global spectral model (T80 model with horizontal resolution of ~1.4°) for a period of 28 years (1982–2009). The main aim of this work is to analyze the capabilities of the RegCM to simulate the wintertime precipitation over North India in the recent past; validation revealed a good improvement in reproducing the precipitation compared to results obtained from the T80 model. This improvement comes due to better representation of vertical pressure velocity, moisture transport, convective heating rate and temperature gradient at two different latitudinal zones. Moreover, orography in the high-resolution RegCM improves the precipitation simulation in the region where sharp orography gradient plays an important role in wintertime precipitation processes. Two bias correction (BC) methods namely mean bias-remove (MBR) and quantile mapping (QM) have been applied on the GCM driven RegCM model simulations. It was found that the QM method is more skillful than the MBR in simulating the wintertime precipitation over North India. A comparison of model-simulated and bias corrected precipitation with observed precipitation at 17 station locations has also been carried out. Overall, the results suggest that when the BC is applied on dynamically downscaled model, it has better skill in simulating the precipitation over North India and this model is a useful tool for further regional downscaling studies.

Key words: North India, winter precipitation, bias correction and downscaling.

1. Introduction

North India (NI), known as the ‘‘wheat bowl” of the country, receives about 25% to 30% of the annual precipitation during winter seasons (December, January and February; DJF). Kalra *et al.* (2008) have shown through their studies that precipitation over this region during winter seasons is very important for Rabi crops, particularly for wheat, as it supplements the moisture and maintains low temperature for the development of the crops. The precipitation in the form of snow over the hilly regions of NI helps in maintaining the glaciers, which serve as the vast storehouse of freshwater supply to millions of people downstream throughout the year through rivers of western Himalayan origin. Therefore, for a country like India that gets more than 80% of its wheat production and fresh water from the north Indian region, the question arises whether strategies of winter-time precipitation prediction that have proved useful elsewhere can be adapted to the exceptionally complex terrain of the Himalayas as well?

Various researchers (Pisharoty and Desai 1956; Mooley 1957; Agnihotri and Singh 1982) have shown that NI receives most of its precipitation due to western disturbances (WDs), which brings out heavy bursts of rain and snow. These WDs are extra-tropical low-pressure systems, which originate in the Mediterranean Sea and move along with subtropical westerlies covering several countries for e.g. Iran, Afghanistan, Pakistan and India. Once their passage is hindered by the Himalayas, they release significant precipitation over the hilly regions and adjoining plains (Mohanty *et al.* 1999). It has been brought out from the studies of Kar and Rana (2014) that the frequency and amplitude of these western disturbances in a given month or season decide if the winter season will experience above or below normal precipitation. Over this region, the winter precipitation process has been relatively less explored due to its limited spatial extent and total amount.

It is well known fact that the coupled general circulation models (GCMs) or atmosphere-only GCMs (AGCMs) are the most important tools to generate monthly to seasonal scale predictions in advance. However, in general, they are unable to represent various regional scale processes because of their coarser resolution (Wang *et al*. 2009, Barnston *et al*. 2010, Kar *et al.* 2011, Zhou *et al.* 2013a, Tiwari *et al.* 2014) and requirement of expensive computational resources. The seasonal (DJF) prediction skill of 14 climate models for a period of 25 years (1980-2004) have been analyzed by Wang *et al.* (2009) and it was found that the models have poor skill with temporal correlation (TC) between observation and multi-model ensemble of 14 GCMs being less than 0.3 in precipitation prediction over the Indian sub-continent. Several recent AGCMs performance have been examined by Barnston *et al.* (2010) for a period of 11 years (1997-2008) and their study shows that these GCMs at seasonal-scale are not able to capture the precipitation variability and they found the ranked probability skill score to be less than 0.01. Kar *et al.* (2011) have investigated the 8-member ensemble of National Centre for Medium Range Weather Forecasting (NCMRWF) global spectral model and shown that on a short and medium-range the model's skill is satisfactory during the Indian monsoon seasons; however, on seasonal scale the performance of the model is poor (with correlation coefficient between observation and model precipitation being less than 0.25). Recently Tiwari *et al.* (2014) have examined the skill of five state-of-the-art GCMs in simulating the inter-annual variability of wintertime precipitation over the NI and found that the models have varying skill. The TC between observed and model precipitation ranged from -0.2 to 0.3. Therefore, it is necessary to study the small-scale physical processes that play important roles in modulating short-term climate over the NI region. Therefore, in the purview of the above discussion, an alternative approach is the dynamical downscaling that is based on nesting of high-resolution regional climate models (RCMs) to

simulate finer scale physical processes consistent with large-scale weather evolution prescribed from a GCM (Giorgi 1990, Jones *et al.* 1995, Giorgi *et al.* 2001, Nobre *et al.* 2001, Rummukainen 2010, Santos *et al.* 2014).

The availability of RCMs has opened up an avenue for more accurate climate predictions in recent decades (Giorgi *et al.* 2001, Christensen *et al.* 2007). However, recent studies (Piani *et al.* 2009, Teutschbein *et al.* 2012) show that these RCMs have varying skills in simulating climatology and inter-annual variability of observed precipitation because of the inherent bias present in them. Piani *et al.* (2009) showed that improvement of forecasts could be made by statistical bias correction (BC) of the Danish Meteorological Institute (DMI) regional model over Europe. Several techniques for BC have been developed (such as Wood *et al.* 2002; Kharin and Zwiers, 2002; Ines and Hansen, 2006; Piani *et al.* 2009). Therefore, in the preview of above discussion RCMs output must be corrected prior to use at the local scale using appropriate bias removal methods. No such studies are available in the context of wintertime precipitation over NI, where attempts have been made to evaluate the skill of different BC techniques.

So, keeping in mind this edge of dynamical downscaling approach over GCM simulations, an attempt has been made to study the downscaling skill of the Regional Climate Model (RegCM) developed at the Abdus Salam International Centre for Theoretical Physics (ICTP) during winter seasons over the NI region. The novelty of the present study lies in the fact that it attempts:

- to find out the skill of dynamically downscaled precipitation simulations;
- to find the plausible reasons for model failure, if any; and
- to find a robust BC method for wintertime precipitation over the NI region

The remainder of this paper is organized as follows. The description of model, experimental design and methodology is provided in Section 2. Discussions on main findings of

the study are presented in Sections 3. The summary and conclusions of the study are given in Section 4.

2. Model, experimental design and methodology

2.1 Model

In the present study, the NCMRWF global spectral model (T80) and ICTP RegCM model have been used. The T80 model is the climate version of the medium-range weather forecast model of NCMRWF, India, which is one of the leading organizations to generate real-time forecast for the Indian region. This is a global spectral model with 80 waves in Triangular truncation (T80) and equivalent to 1.4° × 1.4° horizontal grid resolutions. A fairly basic Kuo-Anthes type of cumulus scheme (Kuo 1974; Anthes 1977) is used to model the deep convection. Further details of the model can be found at Kanamitsu *et al.* (1991), Kar (2007) and Kar *et al.* (2011). The T80 model is atmosphere only model (2-*tier*). Seasonal simulations were carried out forcing the model with forecasted sea surface temperature (SST) from Climate Forecast system, version-2 (CFSv2) of the National Centres for Environmental Prediction (NCEP), USA.

The RegCM (version 4.1.1) used in the present study consists of hydrostatic dynamical core similar to the fifth-generation Pennsylvania State University−National Center for Atmospheric Research Mesoscale Model (MM5) (Grell *et al.* 1994). It is a hydrostatic, terrain following model with state-of-the-art multiple physics options. The other details of the model can be found in Elguindi *et al.* (2011) and Giorgi *et al.* (2012). In the present work the cumulus scheme of Grell (1993) with Fritch–Chappell closure (Fritsch and Chappell 1980), land-surface scheme of Community Land Model or CLM3.5 (Oleson *et al.* 2008), radiative transfer of the NCAR Community Climate Model version 3 (CCM3, Kiehl *et al.* 1996) and nonlocal boundary scheme by Holtslag *et al.* (1990) is used. The model domain and configuration used in this work

are shown in Fig.1 and Table 1 respectively. The rectangular box drawn on Fig. 1 shows the area of interest for which results are analyzed in this study.

2.2 Experimental design

In the present study, the north–south extent of the RegCM model is up to 320 grid points and the east–west extent is up to 416 grid points with center point of the model domain positioned at 15.1^0N/74.5^0E. The model integration is made from 1st November to 28th (29th for a leap year) of February of each year, for a period of 28 years (1982-2009) at 30 km model horizontal resolution. The initial and lateral boundary conditions from NCMRWF global spectral model (T80) have been used. Two sets of downscaling experiments were conducted. The first experiment (RegCM_f) used forecast SSTs from NCEP CFSv2. The second experiment (RegCM_o) used observed SST from the National Oceanic and Atmospheric Administration Optimal Interpolation SST (version 2, NOAA_OISST_V2).

The model-simulated results are validated with the NCEP- Department of Energy (DOE) reanalysis-2 data (hereafter referred to as NNRP2; Kanamitsu *et. al.* 2002), Climatic Research Unit (CRU) gridded precipitation (0.5° × 0.5°) data (Harris et al. 2014), Indian Meteorological Department (IMD) gridded precipitation (0.25° × 0.25°) data (Pai *et al.* 2014) and station level data sets from Snow and Avalanche Study Establishment (SASE). It is to be stressed here that DJF seasonal rainfall data for a year is constructed by taking average of that year's December rainfall and next year's January and February rainfall. For example, values of 1982 DJF seasonal rain is obtained by averaging rainfall values of December 1982, January 1983 and February 1983.

2.3 Methodology

Most of the studies of BC methods have examined the bias corrected rainfall in the purview of climatology and/or root mean square error (RMSE). In the present work, some other skill scores have been introduced to examine all the methods.

BC is generally performed in two ways (i) transformation bias correction (TBC) and (ii) without transformation bias correction (WTBC). In the TBC approach, the biases are removed by constructing a statistical function. On the other hand in the WTBC approach, models are corrected by estimating and adjusting the biases explicitly. A leave-one-out cross-validation technique (recommended by the WMO standardized verification system) has been applied while executing the BC procedures i.e. out of 28 years data (1982–2009) available for this study, each year has been successively withheld from the training dataset, and the remaining 27 years have been used for calculation of all statistics.

2.3.1 Transformation bias correction (TBC)

In this technique, the BC is performed by statistical transformation function such as mapping or fitting between observation and model output. Quantile mapping technique (QM) is used in this study, which is described below:

2.3.1.1 Quantile mapping technique (QM)

A transformation function is used for bias removal in this technique (Wood *et al.* 2002; Ines and Hansen, 2006; Piani *et al.* 2009; Acharya *et al.* 2012). This bias corrected model output is the inverse of cumulative distribution function (CDF) of observed values at the probability corresponding to the CDF of model output at the particular value. For example, suppose mean of model forecast (X_X) and mean of observed data (X_y) are known, then, the bias corrected value QM for $\overline{X_t}$ will be as follows:

$$QM = X_y^{-1}(X_x(X)) \qquad \text{……..(1)}$$

Where, X^{-1} is an inverse of CDF. So, the QM approach is a transformation between two CDFs. Further, a detailed description of this method can be found in Wood *et al.* (2002).

2.3.2 Without transformation bias correction (WTBC)

In this correction procedure, the bias removal is done by without any statistical transformation function. The Mean Bias Removal (MBR) method used here is described below:

2.3.2.1 *Mean Bias Removal technique (MBR)*

This technique is termed as bias-removed individual forecast approach by Kharin and Zwiers (2002). In this approach, the mean bias which is adjusted in every year, is defined as the difference between observed climatology $(\overline{O})$ and model climatology $(\overline{X})$:

$$mbr_t = \overline{O} - \overline{X} \qquad \text{…….(2)}$$

Here the leave-one-out cross-validation approach is used to calculate this difference (mbr_t) for each year and this mean bias is added in the 'test' (t) year's model mean i.e. $MBR_t = \overline{X_t} + mbr_t$. More details of this method are provided in Acharaya *et al.* (2012).

3. Results and discussion

3.1 Simulation of precipitation and circulation climatology

Figure 2 (a) shows the seasonal mean (DJF) precipitation climatology (mm/day) from the CRU gridded dataset. It is seen that the precipitation amount varies from 0.5 to 4 mm/day over Afghanistan, Pakistan and adjoining north India and reduces gradually southward. Fig. 2 (b) shows the precipitation over Indian land point from IMD gridded precipitation data for the period 1982-2009. As this data is available only for the Indian domain, precipitation outside the Indian

boundary is not seen. A precipitation maxima (4 -5 mm/day) is seen over the Kashmir region of NI and the precipitation amount reduces gradually southward. Over the region of interest (marked as rectangular box on Fig. 1), the precipitation occurs due to frequent passages of WDs, and the rainfall variability is coherent. Though the area of interest is north India only (shown in Fig 1), we have provided plots of a larger domain keeping the area of interest in the center for better clarity. Figure 2 (c & d) compares the seasonal mean (DJF) precipitation climatology (mm/day) from the T80 model and the RegCM simulations for the period 1982-2009 (forced by the T80 model). The results over only land points from the T80 and RegCM4 models are shown in the figures. For the sake of brevity, all the results from RegCM_f are described in the following text as RegCM results, unless otherwise so mentioned. Since these precipitation datasets are of different resolutions, the T80 (1.4° × 1.4°) and RegCM (30 km) simulated precipitation are interpolated to those of CRU grids at 0.5° × 0.5° using a simple bilinear interpolation technique. It is seen from Fig. 2 (c) that the T80 model is able to depict the observed features of climatological precipitation up to certain extent spatially, however the model underestimates the precipitation intensity by about 2 mm/day over most parts of the RegCM model domain. Even though, the T80 model is poor in simulating the DJF precipitation climatology, RegCM improved the precipitation simulation (Fig. 2d). However the precipitation is overestimated over north India and adjoining areas of Pakistan. Over the southern continental parts of the model domain, there is negligible rainfall.

Figure 3 (a & b) shows the bias (in %) between the observed and the model (T80 and T80_RegCM) simulated precipitation respectively. The T80 model shows dry bias (Fig. 3a) over most parts of the NI region with maximum dry bias (>160%) over the northwestern parts of Jammu and Kashmir (J&K). On the other hand, a dry bias (>120%) can be noticed (Fig. 3b) over

eastern parts of J&K in T80_RegCM model. Figure 3 (c & d) shows the spatial pattern of root mean square error (RMSE) and correlation between the rainfall anomalies from the T80 model and observations, calculated grid point-wise for the period 1982–2009 respectively. It is seen in Figure 3 (c) that over J&K, Himachal Pradesh (HP) and Uttarakhand (UK) regions, the RMSE values range from 0.5 to 3 mm/day. The maximum RMSE is seen over the northwest Kashmir. Over the western Himalayas parts of India, where the occurrence of rainfall is the maximum compared to other regions during winter seasons, the correlation coefficient (Fig. 3d) is low compared to that over central India, and the RMSE is high (> 1.5 mm/day). RMSE and correlation between the rainfall anomalies from the T80_RegCM and observation are also computed and shown in Figure 3 (e & f). It can be seen in Figure 3 (e) that, the RMSE value ranges between 0.5 to 3 mm/day over most parts of the western Himalayan region with a maximum over eastern part of J&K (> 2 mm/day). Furthermore, it can be noticed from the Figure 3 (f) that the correlation coefficient (CC) is higher compared to the T80 model over NI though it is not statistically significant at 95% confidence level. It is worth mentioning here that for 28 years of data which is analyzed in this study, correlation values greater than 0.38 are statistically significant at 95% confidence level for 2-tailed test. Therefore, over the domain of interest during wintertime (DJF), the T80 model does not have statistically significant correlation. On the other hand, the T80 driven RegCM (T80_RegCM) model simulations has brought out the spatial pattern of observed climatology up to certain extent along with the magnitude of precipitation better compared to the T80 model.

Although the RegCM_o uses prescribed observed SST, it shows marginally less correlation and higher RMSE than RegCM_f simulation with prescribed SST. This result highlights the following facts. The global model (T80) does not respond to interannual variability

of SSTs realistically. Internally generated variability dominates over the SST-forced variability. Therefore, the lateral boundary conditions for the RegCM_o simulations do not correctly represent the atmospheric parameters. The marginal differences in the skill between the RegCM_f and RegCM_o is not significant, indicating that SST may not be playing any important role in the simulations in the area of interest. However, it may be noted that these are only single realizations for each year. A set of ensemble runs are required for obtaining robust differences.

Figure 4 represents the vertical structures of the seasonally averaged zonal and meridional components of wind averaged over a longitudinal belt (from 28ºE to 128ºE). The latitudinal cross-section of the zonal wind from observation (NNRP2), T80 and T80 driven RegCM (hereafter referred as T80_RegCM) model is shown in Figure 4 (top panels; a-c). It is noticed that upper air westerly jet stream (WJS) is well represented in both (T80 and T80_RegCM) model simulations, though, the area with core WJS and its strength is close to the observation in T80_RegCM simulations compared to the T80 model. Fig. 4 (bottom panel; d-f) also shows the sectorial average of meridional component of wind. The diagram depicts that at upper pressure levels (from 200-100 hPa) this component of wind is also well brought out by the T80_RegCM model simulations as compared to the T80 model. It is also noticed that the areas with stronger meridional winds are shifted northward (about 5^{o} shift in northward direction) in T80_RegCM simulations compared to that in the NNRP2. Overall, the T80_RegCM model simulations are closer to observations in terms of intensity, location and pattern of the zonal as well as meridional components wind than the T80 model.

The horizontal resolution of NCEP reanalysis 2 (2.5°) is too coarse to compare T80 (1.4°) and RegCM (30 km). In Fig. 4, the vertical structure of climatological zonal and meridional winds for DJF have been compared. Chelliah *et al.* (2011) have compared the vertical structure of winds

from CFSR against NCEP reanalysis-1, NCEP reanalysis-2 and the European Centre for Medium Range Weather Forecasting (ECMWF) reanalysis-40 (ERA40) reanalysis. They have concluded that the climatological zonal mean winds for both the winter three month seasons from CFSR are generally in close agreement with NCEP reanalysis-1, NCEP reanalysis-2 and ERA40 reanalyses in the subtropical, middle and high latitudes of both hemispheres. However, systematic differences are found mainly in the deep tropics and near the Polar regions. In this study, the model (T80 and RegCM) results have not been compared against CFSR reanalysis.

3.2 Composite Analysis

Although the performance of T80_RegCM model simulations are better compared to T80 model but that is on climatological scale. Therefore, for gaining more insight on model simulations of precipitation, interannual variability of simulated precipitation has been compared against the observed variability. Observed and model simulated (T80 and RegCM) wintertime precipitation anomalies over NI region for each year are shown in Figure 5. The signs of rainfall anomalies from the T80 model simulation for most of the wet as well as dry years do not match with that of observed anomalies. Further, the TC for T80 and RegCM over the region of interest has been computed. The TCs for T80 and RegCM are 0.22 and 0.36 respectively, which shows a clear improvement from T80 to RegCM4 simulation. It is also evident from the Figure 5 that, though both RegCM simulations ($RegCM\_o$ and $RegCM\_f$) show higher skill in predicting rainfall anomalies for the wet and dry years compared to the T80 model, there is very little difference between them over NI region for each year. From the seasonal mean precipitation anomalies, extreme years (wet/dry) are selected from the observed precipitation data of India Meteorological Department (IMD) on the basis of their departure form mean i.e. years having standardized precipitation anomaly greater than 1 mm/day are considered as wet, while years having less than -

1 mm/day standardized precipitation anomaly are considered as dry years. Therefore, out of 28 years, there are 4 years in the category of wet (1991-92, 1994-95, 1995-96, 1997-98) and 4 dry (1984-85, 1996-97, 2000-01, 2008-09) years. It may be noted that precipitation anomaly in 2007-08 is lower than that in 1984-85. However, 2007-08 has not been included to make dry- year composite in order to select a year from 1980's so that a dry-year is included from each decade (at least one year from 1980s, 1990s and 2000s). Futher the composite results will not change much if 2007-08 is included. A composite analysis has been carried out by computing the precipitation anomaly pattern during wet/dry precipitation years.

Figure 6 (a-c) shows observed and model simulated precipitation difference (in %) between wet and dry years. It is noticed that over most parts the domain of interest, a coherent positive precipitation pattern has emerged and this positive difference lies in the range of 20% to 30% in the observation (Fig. 6a). This observed precipitation is well brought by the T80_RegCM model simulation compared to the T80 model, which underestimates the precipitation amount and shows a negative difference of about 10% to 20 % over Punjab and Himachal Pradesh regions of NI. In case of composite analysis of winds (at 500 hPa) shown in Fig. 7 (a-c), the observation has anomaly of stronger westerlies (~ 3 m/s) over central part of India succeeded by cyclonic flow due to hindrance of the great Himalayan orography. As previously mentioned, the northern part of India receives precipitation when WDs passes over the region forming cyclonic anomaly over J&K and adjoining regions. The T80_RegCM model simulation is able to bring out the observed cyclonic flow feature better compared to the T80 model.

The differences in orography of T80 and RegCM models are due to difference in horizontal resolution (figure not shown). Higher peaks as well as valleys are noticed over the northwest Himalayan region more clearly in the RegCM than in T80 model. It is worth

mentioning here that the Himalayan topography is characterized by strong north-south gradient. Though the RegCM model shows topographical features of the Himalayan region better than T80 model, the RegCM model does not represent the real mountain peaks (due to the fact that resolution of RegCM is still to coarse to resolve the sharp gradient in orography of the region) and hence does not fully captures the actual topographical gradient of the Himalayas. Over all, the RegCM model represents the shape of the orographic barriers (which has the dominant role in enhancing precipitation by orographic lifting over mountainous region) more clearly compared to T80 model. Therefore, when RegCM model orography is used in model simulations, the spatial pattern and intensity of precipitation around topography becomes sharper and the spatial extent of precipitation seen in the T80 model is improved.

It may also be noted that, the T80 model uses a fairly basic Kuo-Anthes type of cumulus scheme (Kuo 1974; Anthes 1977) to model the deep convection. In the present study, the RegCM4 model uses the cumulus scheme of Grell (1993) with Fritch–Chappell closure (Fritsch and Chappell 1980). Sinha *et al.* (2014) have examined the performance of the RegCM4 model with various convective parameterization schemes in simulating winter circulation and associated precipitation over the Western Himalayas. It was found that the atmosphere is colder over northern India and the Himalayas than in the southern parts of India during excess rainfall years than the deficient rainfall years. The temperature gradient persists from the south to the north where the isotherm lines are oriented in nearly east–west directions in the upper air over India and its adjoining area in excess years. The pattern and magnitude of the upper air temperature and its gradient are sensitive to the cumulus scheme chosen. The Grell cumulus scheme with Fritsch Chappell closure (Grell-FC) has performed better in RegCM simulations compared to other schemes. In the Grell scheme, clouds are considered as two steady-state circulations, a downdraft

and an updraft. The cloudy air and the environment mix only at the top and bottom of the cloud. Along the edges of the cloud no entrainment or detrainment is allowed, and the mass flux of the clouds does not vary with height. The FC closure assumes that clouds remove the available buoyant energy for convection in a given timescale. The T80 model does not have elaborate treatment of convection suitable for highly inhomogeneous high terrain regions. Therefore, in addition to better representation of topography, convection scheme in the RegCM model play important role for better simulations than the T80 model.

The vertical pressure velocity (hereafter referred as omega) is one of the important upper air parameter that plays an important role in the model dynamics for precipitation simulation. Hence, it would be interesting to study the performance of T80 and T80_RegCM model in simulating the omega field. The longitude, height vertical cross-section of the differences between seasonal mean (DJF) wet- and dry-year composites of vertical pressure velocity at 35^{o} N is shown in Fig. 8 (a-b). The orography of both the T80 and RegCM simulations are also shown (in the black shaded bar). It can be noticed in Fig. 8 that the vertical velocity maxima/minima is either along the upslope side of topography or over the valley bottom, which shows that the influence of the ridge–valley system on the vertical motion and hence precipitation formation processes. These vertical distributions across the Himalayan region are more clearly brought out in RegCM simulations compared to T80 model. This increased vertical motion could be one of the reasons for producing more (less) precipitation in RegCM than the T80 model during wet (dry) years.

Furthermore omega field obtained at 500 hPa from NNRP2 reanalysis, T80 and T80_RegCM model simulations has been analyzed (figure not shown). It is noticed that during winter seasons, negative omega prevails over western parts of Himalaya in the observations (reanalysis). The model simulations (both the T80 and T80_RegCM) are able to bring out the

negative omega over the region, though the areal extent of this negative omega is less in the both the models as compared to the observed data (reanalysis). The area with stronger omega field over that region is represented better in the T80_RegCM simulation compared to the T80 model.

The difference between wet and dry year composites of seasonal mean (DJF) vertical integrated moisture fluxes and transport from observation, T80 and T80 driven RegCM simulations are shown in Fig. 9 (a-c) respectively. It can be noticed from the diagram that both the model simulations (T80 and T80_RegCM) show large-scale moisture fluxes, with stronger transport from westerly directions. Further in both the model simulations, a high flux convergence over and across high orographical regions and a weaker flux convergence or even divergent fluxes over and along valley regions can be seen. Furthermore investigation indicates that the spatial distribution in composite analysis is present in more detail in the RegCM simulations compared to that in T80. This could be due to the coarser resolutions of T80 and difference between T80 and RegCM topography.

Yanai *et al.* (1973) have shown through their study that most of the rain in tropics consists of a combination of convective and stratified form clouds. Therefore, to get a deep insight on possible reason affecting the model performance, convective heating rates are computed and their corresponding vertical profiles are shown in Figure 10 (a). It can be noticed from the figure that the maximum convective heating rate is at 400 hPa in NNRP2 reanalysis (4.1ºC/day). The T80_RegCM model is able to bring out this convective heating rate (4.7ºC/day) better compared to T80 model (2.7ºC/day) at 400 hPa level. Overall, due to better representation of convective heating rates the simulation of precipitation is better in the T80_RegCM experiment compared to the T80 model. The temperature gradient between two latitudinal circles (40°N - 45°N & 25°N – 30°N) has been computed and shown in Fig. 10 (b). It is seen that between 75°E and 90°E, the

temperature gradient is less in observation and RegCM compared to the T80 model. It suggests that in case of T80 model more cold/dry air intrusion from higher to lower latitudes, which in turn leads a drying and underestimation of precipitation. On the other hand, in case of T80_RegCM the gradient is low which results in less dry air intrusion from the higher latitudes that in turn leads to more precipitation.

3.3 Bias Correction

To examine how well the distribution of model-simulated values corresponds to the distribution of observed values, a box-whisker plot (Fig. 11a) has been drawn for domain of interest. Boxes indicate the 25th to 75th percentiles of the distribution, while the whiskers show the full width of the distribution. It can be noticed that the distribution of the QM values are closer to the distribution of observed values compared to T80, T80_RegCM model and MBR method itself. Equitable Threat Score (ETS) for Yes/No categorical forecast (Gilbert, 1884 and Wilks, 1995) is defined as:

$$ETS = \frac{(C - C_l)}{(C + M + F_a - C_l)} \text{ , where } C_l = \frac{(C + M)' (M + F_a)}{N} \qquad \ldots\ldots\ldots\ldots (3)$$

Here, M, C and F_a are the number of misses, the number of hits and the number of false alarms for each category respectively. The hits due to random chance are denoted by C_l and N is the total number of events. The ETS lies in the range of −0.33 to 1. ETS = 0 indicates no skill and ETS = 1 indicates perfect skill in prediction. As the maximum values of precipitation from the observation during the study period (1982–2009) vary from 3 to 4 mm/day, three thresholds, 3, 3.5 and 4 mm/day have been considered for calculating ETS. Fig. 11 (b) shows the ETS values of T80, T80 driven RegCM with observed and forecasted SST (RegCM_$_o$ and RegCM_$_f$) and two

bias corrected methods (QM and MBR). It can be noticed from the diagram that for all the thresholds ETS values of QM is higher than T80, T80 driven RegCM model and MBR method.

A Taylor diagram (Taylor, 2001) is presented in Figure 12. In this diagram, the skill of the T80 model, T80 driven RegCM with observed and forecasted SST (RegCM_$_o$ and RegCM_$_f$) and two bias corrected methods (QM and MBR) for prediction of rainfall during winter in terms of correlation, root mean square error (RMSE) and standard deviation is shown. The figure clearly depicts that the QM method shows significant correlation skill with less RMSE as compared to the T80, T80_RegCM model and MBR method.

3.4 Validation of model precipitation with station observations

In this section, the T80, T80_RegCM models and two bias corrected methods (QM and MBR) are validated against the observations over seventeen stations located over the North Indian part of the Western Himalayas (IWH) region (Tiwari *et al.* 2015). These observed station datasets are obtained from Snow and Avalanche Study Establishment (SASE), Chandigarh. The gridded precipitation datasets obtained from T80, T80_RegCM and two bias corrected methods (QM and MBR) are bi-linearly interpolated to the station location for validation. Station data is used instead of CRU/IMD dataset as both the precipitation datasets are based on observed data from the same set of observing stations/rain gauges. These datasets are available at 0.5°×0.5° in CRU and 0.25°×0.25° resolution in case of IMD. IMD observing stations in the western Himalayan region are very few. Observing stations installed and operated by SASE are not included in the IMD or CRU gridded precipitation data. Therefore, SASE observations are additional source of rainfall information in the region. Moreover, in order to avoid any error in interpolation and station data being the truth, SASE station data are used to validate the model precipitation over region of interest. Table 2 represents the station–wise seasonal mean precipitation obtained from SASE

observation, T80, T80_RegCM and two bias corrected methods. The shaded values of model simulation and bias corrected method indicate the closest ones to the SASE observations. Further to a get deep insight, the Phase synchronizing events (PSE) has been computed for the performance evaluation based on Table 2 results. The PSE method matches the sign (positive or negative) of the precipitation difference (composite of wet minus composite of dry years) obtained from observations (data from SASE stations) and the T80, T80_RegCM and two bias corrected methods (QM and MBR) to evaluate the performance of the model.

The computation of PSE is given below:

$$PSE = \left(\frac{T_e - T_e'}{T_e}\right) 100 \qquad \text{.....(4)}$$

where T_e is the total number of events and T_e' is the number of events in the T80, T80_RegCM and two bias corrected methods (QM and MBR) that have opposite in sign as compared to observations (out of phase). Thus, PSE=100 for the T80, T80_RegCM and two bias corrected methods (QM and MBR) results means that the sign of model anomalies (here the difference from composite of wet and dry years) is same as in the observations for all the stations and PSE=0 when none of the model results have a similar sign (i.e. either positive or negative both in model and observation) with observations. From the Table 2, it can be seen that the PSE value is maximum (with 94%) for composite (i.e., model output matches the sign of with observations 94% times) of wet minus dry years for QM method followed by MBR method (with 82%), T80_RegCM (with 71%) and T80 model (with 59%). Therefore, it can be concluded that bias corrected QM method is able to represent the precipitation pattern and intensity with high fidelity compared to MBR, T80_RegCM and T80.

3.5 WD case study

As explained in Section 1, WDs are synoptic weather systems that deliver much of the winter precipitation over the NI region. Therefore, with an objective to see whether WD is also improved in the RegCM simulation compared to T80 model itself, an intense WD case (13 - 17 January 2002) is considered. Fig. 13 depicts observed, T80 and RegCM model simulated streamlines (at 500 hPa) and precipitation for an intense WD that occurred during 13 - 17 January 2002. The observational analysis shows that on 15th January (Fig. 13 a3), there was a well-marked trough at 500 hPa in the mid tropospheric westerlies nearly along longitude 68°E and north of latitude 27°N. This trough further moved eastwards on 16th and 17th respectively (Fig. 13 a4 & a5). During this period a precipitation belt can be seen in the observation confined mainly over the Indian parts of western Himalayas (WH) and adjoining plains. In case of the T80 model, the structure of mid tropospheric westerlies does not agree well with that from observation and it underestimates the precipitation amount (Fig. 13 b6-b10) over WH and adjoining plains. On the other hand, the RegCM model simulations (Fig. 13 c1-c10) generally agree well with the observed flow patterns though it over-predicts the heavy precipitation amounts over the northern plains.

Further an attempt has been also made to assess orographical forcing and the precipitation-forming mechanism during 13 - 17 January 2002. For this purpose the cross-sectional distribution (at 35°N) of vorticity, relative humidity and topography is plotted and shown in Fig. 14. A detailed analysis of the diagram suggests that the vertical deflection of flow induced by the topography results in adiabatic cooling, and with sufficient moisture forms cloud and hence precipitation over the region. Convergence on the upslope due to decreased velocity through orographic retardation slows down the flow and results in generating a mid-troposphere positive vorticity during the peak of the storm (Fig. 14 b and c). Moreover, positive vorticity prevails over

the leeward and valley floors while a weaker negative vorticity (Fig. 14) along the orographic surface toward the windward side. The effects of strong ridge-valley flows can be summarized in two-fold: (i) the strong valley flow reduces the upslope moisture flow, and (ii) valley boundaries provide suitable conditions for precipitation formation. Overall, the analysis reflects the models' robustness at the event scale and paves a path of using dynamic downscaling methods in basin scale studies.

4. Conclusion

The downscaling experiment over North India (NI) has been conducted by forcing the RegCM with the NCMRWF global spectral model simulation output for a period of 28 years (1982–2009) at a horizontal resolution of 30 km. The winter season climate is first compared with observations to study the downscaling skill of the RegCM over the NI. The results indicate that the wintertime climatology of precipitation, upper airfields at different pressure levels, and the interannual variability is more accurately simulated by the T80 driven RegCM (T80_RegCM) than the T80 model itself. Composite analysis for extreme precipitation years suggests that the precipitation and circulation feature simulated by the T80_RegCM shows better skill compared to T80. A complete and statistically robust analysis also suggests that downscaling provides a credible means to improve GCM climate simulations. The major findings of the study are enumerated as follows:

- The T80 model, in general, underestimates the observed climatology and IAV of precipitation. On the other hand T80_RegCM simulation has brought out the observed climatology and IAV better than the T80 model though it shows a wet bias over domain of interest.

- A composite analysis has been carried out for precipitation by computing the precipitation anomaly pattern during wet/dry years. The composite analysis reflects that T80_RegCM simulation is able to bring out the rainfall and upper air wind anomaly reasonably well and close to observation as compared to T80 model itself.
- To understand the possible reasons which are affecting the performance of the T80 and T80_RegCM model simulations orography representation, vertical pressure velocity, moisture transport, convective heating rate and temperature gradient at two different latitudinal circles are analyzed and it is seen that these factors influence the rainfall during winter season over NI region. While T80_RegCM model is able to demonstrate the above said features up to certain extent, the T80 model does not represent those features in a realistic manner.
- Two BC techniques have been used and it has been found that the Quantile mapping (QM) method is more skillful than the Mean bias-remove *(*MBR). The reason behind the better skill of QM over MBR technique is that it's a sophisticated technique based on statistical transformation, while the later one is a simple method, where the mean bias is adjusted in every year.
- The skill of bias corrected (BC) approaches have been examined against non bias corrected (NBC) on station levels and it is found that the bias corrected QM method is able to represent the precipitation amount with high fidelity compared to MBR, T80 and T80_RegCM.
- Further, with an objective to see whether WD is also improved in the RegCM simulation an intense WD case has been selected. The analysis revealed that the RegCM is able to simulate the flow field and associated precipitation reasonably well.

It should be mentioned that downscaling of one ensemble member can be considered a limitation for drawing robust conclusions for the predictive skill of the two BC methods and their comparison. Although computationally expensive, using a large number of ensembles are needed for a more critical evaluation. Our next study on downscaling of precipitation will be improved by applying multiple ensemble runs with a sufficiently longer period.

Acknowledgements

We thank the anonymous reviewers for their comments and suggestions that helped us to improve the manuscript. The RegCM4.1.1 model, installed at IIT Delhi, was developed at the ICTP, Trieste, Italy. Authors sincerely acknowledge the IMD and SASE for providing their daily gridded and station precipitation data. The authors would like to acknowledge NCEP for reanalysis 2 data provided by the NOAA/OAR/ESRL PSD, Boulder, Colorado, USA, from their Web site at http://www.esrl.noaa.gov/psd/. The work is partly supported by research grant from Department of Science and Technology, Govt. of India under contract DST/CCP/PR/11/2011 through a research project operational at IIT Delhi (IITD/IRD/RP2580). The authors duly acknowledge Bianca C. for editing the English of the manuscript. The authors wish to thank three anonymous reviewers whose comments served to improve the clarity and coherence of this manuscript.

References

Acharaya N, Chattopadhayay S, Mohnaty UC, Dash SK, Sahoo LN. 2012. On the bias correction of general circulation model output for Indian summer monsoon. *Met. Appl*. **20**: 349-356.

Anthes RA. 1977. A cumulus parameterization scheme utilizing a one- dimensional cloud model. *Mon. Weather Rev.* **105**: 270–286.

Agnihotri CL, Singh MS. 1982. Satellite study of western disturbances. *Mausam*. **33**: 249–254.

Barnston AG, Li S, Mason SJ, DeWitt DG, Goddard L, Gong X. 2010. Verification of the first 11years of IRI's seasonal climate forecasts. *J. Appl. Meteorol. Clim*. **49**: 493–520.

Chelliah M, Ebisuzaki W, Weaver S, Kumar A. 2011. Evaluating the tropospheric variability in National Centers for Environmental Prediction's climate forecast system reanalysis. *J. Geophys. Res.* **116**: D1710, doi:10.1029/2011JD015707.

Christensen JH, Carter TR, Rummukainen M. 2007. Evaluating the performance and utility of regional climate models: the PRUDENCE project. *Clim. Change.* **81**: 1-6.

Dickinson RE, Henderson-Sellers A, Kennedy PJ. 1993. Biosphere-Atmosphere Transfer Scheme (BATS) version 1e as coupled to the NCAR Community Climate Model. *NCAR Tech. Note NCAR/TN-387+STR, 72 pp*.

Elguindi N, Bi XQ, Giorgi F, Nagarajan B, Pal J, Solmon F, Rauscher S, Zakey A, Giuliani G. 2011. Regional climatic model RegCM user manual version 4.1.1, The Abdus Salam International Centre for Theoretical Physics Strada Costiera, Trieste, Italy.

Fritsch JM, Chappell CF. 1980. Numerical prediction of convectively driven mesoscale pressure systems, part 1: Convective parameterization. *J. Atmos. Sci.* **37**: 1722–1733.

Gilbert GK. 1884. Finley's tornado predictions. *Am. Meteorol. J.* **1:** 166 –172.

Giorgi F. 1990. Simulations of regional climate using a limited area model nested in a general circulation model. *J. Clim*. **3**(9): 941-963.

Giorgi F, Hewitson B, Christensen H, Hulme M, Von Storch H, Whetton P, Jones R, Mearns L O, Fu G. 2001. Regional climate information evaluation and projections, Climate Change: the scientific basis. *Cambridge University Press*. pp. 583-638.

Giorgi F, Coppola E, Solmon F, Mariotti L, Sylla MB, Bi X, Elguindi N, Diro GT, Nair V, Giuliani G, Cozzini S, Gu¨ttler I, O'Brien TA, Tawfik AB, Shalaby A, Zakey AS, Steiner AL, Stordal F, Sloan LC, Brankovic C. 2012. RegCM4: model description and preliminary tests over multiple CORDEX domains. *Clim. Res.* **52**: 7–29.

Grell GA. 1993. Prognostic evaluation of assumptions used by cumulus parameterization. *Mon. Weather Rev.* **121**: 764–787.

Grell GA, Dudhia J, Stauffer DR. 1994. Description of the fifth generation Penn State/NCAR Mesoscale Model (MM5*). Tech Rep TN-398+STR, NCAR, Boulder, Colorado, pp.1-121*.

Harris I, Jones PD, Osborn TJ, Lister DH. 2014. Updated high-resolution grids of monthly climatic observations - the CRU TS3.10 Dataset. *Int. J. Climatol.* **34**: 623-642

Holtslag AAM, De Bruijn EIF, Pan HL. 1990. A high-resolution air mass transformation model for short-range weather forecasting. *Mon. Weather Rev.* **118**: 1561–1575.

Ines AVM, Hansen JW. 2006. Bias correction of daily GCM rainfall for crop simulation studies. *Agric. for. Meteorol.* **138:** 44–53.

Jones RG, Murphy JM, Noguer M. 1995. Simulation of climate change over europe using a nested regional-climate model. I: Assessment of control climate, including sensitivity to location of lateral boundaries. *Q. J. R. Meteorol. Soc*. **121**: 1413-1449.

Kanamitsu M, Alpert JC, Campana KA, Caplan PM, Deaven DG, Iredell M, Katz B, Pan HL, Sela J, White WH. 1991. Recent changes implemented into the global forecast system at NMC. *Weather Forecast.* **6**: 425–435.

Kanamitsu M, Ebisuzaki W, Woollen J, Yang SY, Hnilo JJ, Fiorino M, Potter GL. 2002. NCEP-DEO AMIP-II Reanalysis (R-2). *Bull. Am. Met. So.c* **83**:1631–1643.

Kalra N, Chakraborty D, Sharma A, Rai HK, Jolly M, Chander S, Kumar PR, Bhadrary S, Barman D, Mittal RB, Lal M, Sehgal M. 2008. Effect of increasing temperature on yield of some winter crops in northwest India. *Current Science* **94**(1): 82-88.

Kar SC. 2007. Global model simulations of interannual variability of the Indian summer monsoon using observed SST variability. *NCMRWF research Report, NMRF/RR/2/2007; 40 pp.*

Kar SC, Iyengar GR, Bohra AK. 2011. Ensemble spread and model systematic errors in the monsoon rainfall forecasts using the NCMRWF global ensemble prediction system. *Atmosfer.* **24** (2): 173–191.

Kar SC, Rana S. 2014. Interannual variability of winter precipitation over northwest India and adjoining region: impact of global forcing's. *Theor. Appl. Climatol.* DOI 10.1007/s00704-013-0968-z.

Kharin VV, Zwiers FW. 2002. Notes and correspondence: climate predictions with multi-model ensembles. *J. Clim.* **15:** 793–799.

Kiehl JT, Hack JJ, Bonan GB, Boville BA, Briegleb BP, Williamson DL, Rasch PJ. 1996. Description of the NCAR Community Climate Model (CCM3). *NCAR Tech. Note NCAR/TN- 420+STR, 152 pp.*

Kuo YH. 1974. Further studies of the parameterization of the influence of cumulus convection of large-scale Flow. *J. Atmos. Sci*. **31**: 1232–1240.

Mohanty UC, Madan OP, Raju PVS, Bhatla R, Rao PLS. 1999. A study on certain dynamic and thermodynamic aspects associated with Western Disturbances over northwest Himalaya, The Himalayan environment. *New Age International Publishers*. 113-122.

Mooley DA. 1957. The role of western disturbances in the production of weather over India during different seasons. *Indian J. Meteor. Geophys.* **8**: 253–260.

Nobre P, Moura AD, Sun L. 2001. Dynamical downscaling of seasonal climate prediction over Nordeste Brazil with ECHAM3 and NCEP's regional spectral models at IRI. *Bull. Amer. Meteor. Soc*. **82**: 2787–2796.

Oleson KW, Niu GY, Yang ZL, Lawrence DM, Thornton PE, Lawrence PJ, Stöckli R, Dickinson RE, Bonan GB, Levis S, Dai A, Qian T. 2008. Improvements to the Community Land Model and their impact on the hydrological cycle. *J. Geophys. Res.* **113**: 1021-1026.

Pal JS, Giorgi F, Bi X, Elguindi N, Solmon F, Gao X, Rauscher SA, Francisco R, Zakey A, Winter J, Ashfaq M, Syed F, Faisal S, Bell JL, Diffenbaugh NS, Karmacharaya J, Konare A, Martinez D, Da Rocha RP, Sloan LC, Steiner AL. 2007. Regional climate modeling for the developing world: The ICTP RegCM3 and RegCNET. *Bull. Amer. Meteor. Soc.* **88**: 1395–1409.

Pai DS, Sridhar L, Rajeevan M, Sreejith OP, Satbhai NS, Mukhopadhyay B. 2014. Development of a new high spatial resolution (0.25° × 0.25°) long period (1901-2010) daily gridded rainfall data set over India and its comparison with existing data sets over the region. *Mausam.* **65**: 1–8.

Piani C, Haerter JO, Coppola E. 2009. Statistical bias correction for daily precipitation in regional climate models over Europe. *Theor. Appl. Climatol.* **99:** 187–192.

Pisharoty PR, Desai BN. 1956. Western disturbances and Indian weather. *Indian J. Meteor. Geophys.* **8**: 333–338.

Rummukainen M. 2010. State-of-the-art with regional climate models. *WIREs Climate Change.* **1**: 82-96.

Santos e Silva CM, Silva A, Oliveira P, Lima KC. 2014. Dynamical downscaling of the precipitation in Northeast Brazil with a regional climate model during contrasting years. Atmosph. Sci. Lett., **15**: 50–57.

Sinha P, Tiwari PR, Kar SC, Mohanty UC, Raju PVS, Dey S, Shekhar MS. 2014. A sensitivity study on convective schemes towards model resolution in the simulation of winter

circulation and precipitation over the western Himalayas. *Pure and Appl. Geophy.* **172**: 503-530.

Taylor KE 2001. Summarizing multiple aspects of model performance in a single diagram. *J. Geophys. Res.* **106**: 7183–7192.

Teutschbein C, Seibert J. 2012. Bias correction of regional climate model simulations for hydrological climatechange impact studies: review and evaluation of different methods. *J. Hydrol.* **29**: 456–457.

Tiwari PR, Kar SC, Mohanty UC, Kumari S, Sinha P, Nair A, Dey S. 2014. Skill of precipitation prediction with GCMs over north India during winter season. *Int. J. Climatol.* **34**: 3440-3455.

Tiwari PR, Kar SC, Mohanty UC, Dey S, Kumari S, Sinha P, Raju PVS, Shekhar MS. 2015. Simulations of tropical circulation and winter precipitation over north India: An application of a tropical band version of Regional Climate Model (RegT-Band). *Pure and Appl. Ghephy*. DOI 10.1007/s00024-015-1102-1.

Wang B, Lee J-Y, Kang I-S, Shukla J, Park C-K, Kumar A, Schemm J, Cocke S, Kug J-S, Luo J-J, Zhou T, Wang B, Fu X, Yun W-T, Alves O, Jin EK, Kinter J, Kirtman B, Krishnamurti T, Lau N, Lau W, Liu P, Pegion P, Rosati T, Schubert S, Stern W, Suarez M, Yamagata T. 2009. Advance and prospectus of seasonal prediction: assessment of the APCC/CliPAS 14-model ensemble retrospective seasonal prediction (1980–2004). *Clim Dyn*. **33**: 93–117.

Wilks DS. 1995. Statistical Methods in the Atmospheric Sciences. Academic Press: San Diego, CA; 467 pp.

Wood AW, Maurer EP, Kumar A, Lettenmaier DP. 2002. Long-range experimental hydrologic forecasting for the eastern United States. *J. Geophys. Res.* (*Atmos.*) **107** (D20)**:** 4429, doi:10.1029/2001JD000659.

Yanai M, Esbensen S, Chu JH. 1973. Determination of bulk properties of tropical cloud clusters from large scale heat and moisture budgets. *J. Atmos. Sci.* **30**: 611-627.

Zhou TJ, Song FF, Chen XL. 2013a. Historical evolution of global and regional surface air temperature simulated by FGOALS-s2 and FGOALS-g2: How reliable are the model results? *Adv. Atmos. Sci.* **30**(3): 638–657.

List of Figures

Figure 8. Longitude–height distribution of the differences between seasonal mean (DJF) wet- and dry-year composites of vertical velocity (Pa/s; shaded and broken contour) and topography (*1e-3 m; shaded bar, right-hand vertical axis) in (a) T80 and (b) RegCM at 35°N latitude.

Figure 9. The difference between seasonal mean (DJF) wet- and dry-year composites of vertical integrated moisture flux (shaded) and transport (streamlines) in (a) observation, (b) T80, and (c) T80 and T80 driven RegCM (T80_RegCM) simulations, respectively.

Figure 10. (a) Seasonal (DJF) mean convective heating rate (^{0}C/day) computed from NNRP2, T80 and T80 driven RegCM (T80_RegCM) models respectively; (b) Temperature gradient between two latitudinal circles (40^0 N - 45^0 N & 25^0 N – 30^0 N).

Figure 11. (a) Distribution of observed and model simulated precipitation (mm/day) for winter season. (b) Equitable threat score (ETS) computed for T80_RegCM and two bias correction methods (QM & MBR) for winter season.

Figure 12. Taylor diagram for the north India average precipitation prediction skill of the T80, T80 driven RegCMs and two bias correction methods.

Figure 13. Observed, T80 and RegCM simulated streamline and precipitation analysis for an extreme WD case occurred during 13–17 January 2002. The upper panel shows the observed streamlines at 500 hPa (a1-a5) and precipitation (a6-a10). T80 simulated streamlines at 500 hPa (b1-b5) and precipitation (b6-b10) are shown in middle panels. The lower panels shows RegCM simulated streamlines at 500 hPa (c1-c5) and precipitation (c6-c10) respectively.

Figure 14. Longitude–height distribution of vorticity (*1e-5/s; shaded), relative humidity (%; broken contour), and topography (*1e-3 m; shaded bar, right-hand vertical axis) on (a) 12 January 2002, (b) 13 January 2002, (c) 14 January 2002, (d) 15 January 2002, (e) 16 January 2002, and (f) 17 January 2002 at 35°N latitude in the RegCM simulation.

List of Tables

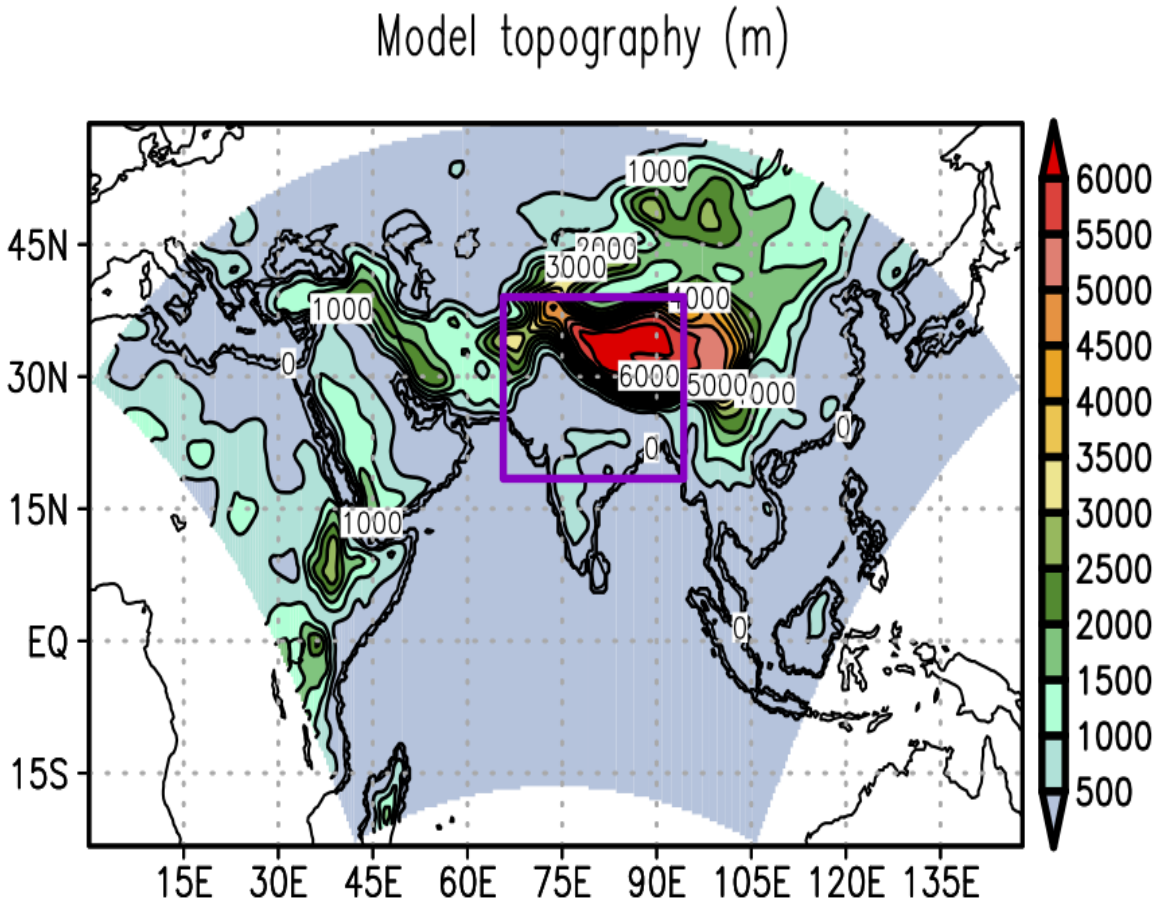

Figure 1. Topography (in m) and full model domain as used in RegCM. The region under the purple box is the north India region considered in the study.

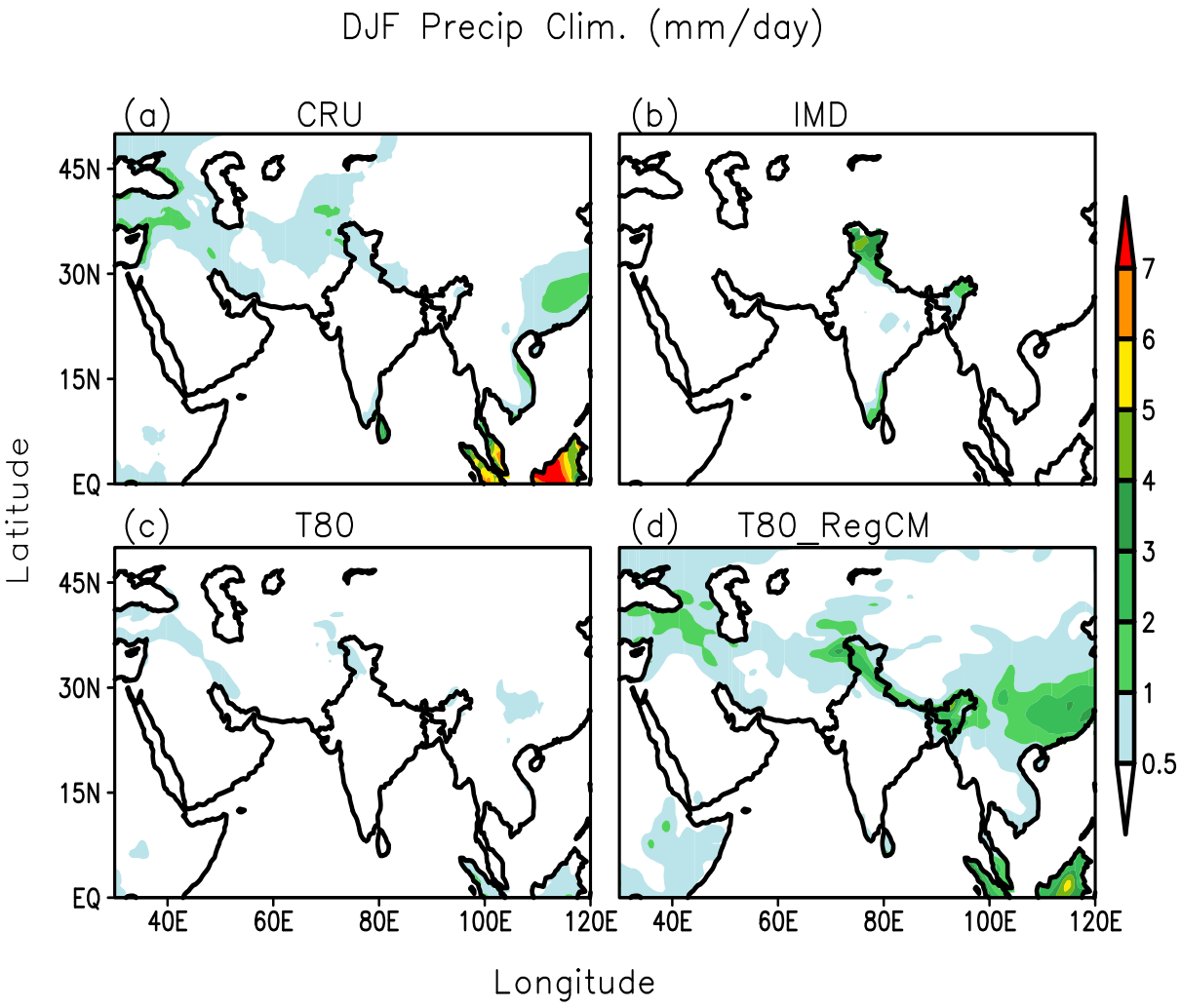

Figure 2. Averaged (1982-2009; DJF) precipitation (in mm/day) from (a) CRU observations, (b) IMD gridded precipitation, (c) NCMRWF GCM (T80) and (d) T80 driven RegCM (T80_RegCM). The results over only land points from the T80 and RegCM4 models are shown in panel (c) and (d) respectively.

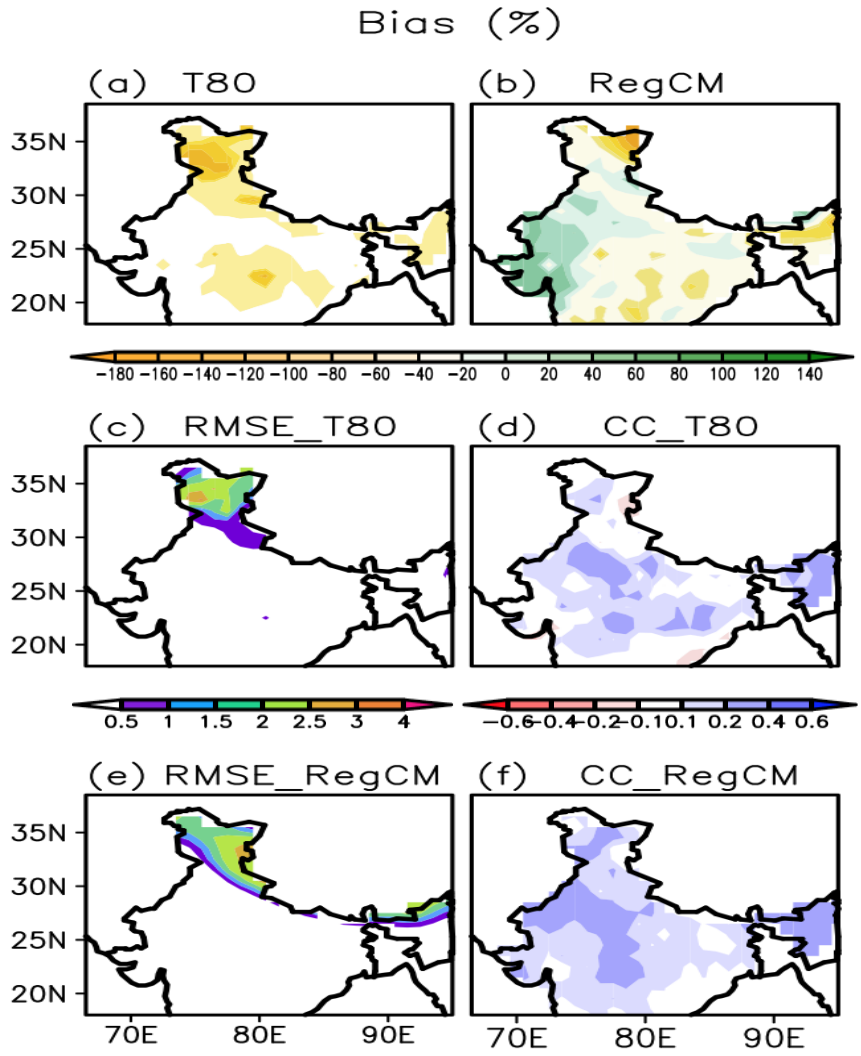

Figure 3. Precipitation bias (from 1982 to 2009 for December to February) with respect to IMD (in %) form (a) NCMRWF GCM (T80) and (b) T80 driven RegCM (T80_RegCM), (c) root mean square error (mm/day) and (d) correlation pattern for T80**.** Panel (e) and (f) are same as (c) and (d) but for T80 driven RegCM.

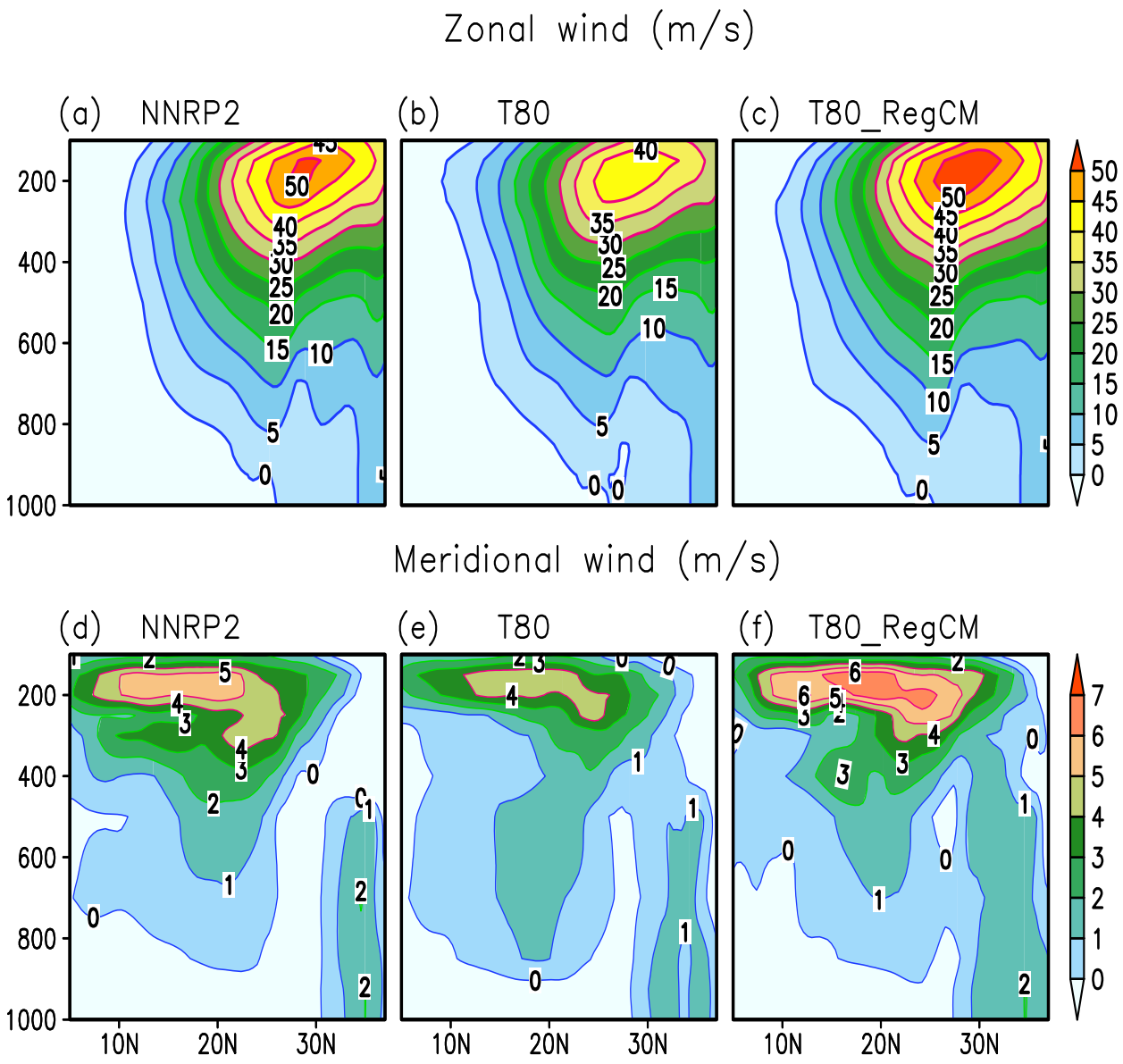

Figure 4. Sectorial (28ºE-128ºE) zonal and meridional climatological winter season wind (in m s^{-1}) of (a) NNRP2, model simulations using (b) NCMRWF GCM (T80) and (c) T80 driven RegCM (T80_RegCM); d, e and f are same as a, b and c respectively.

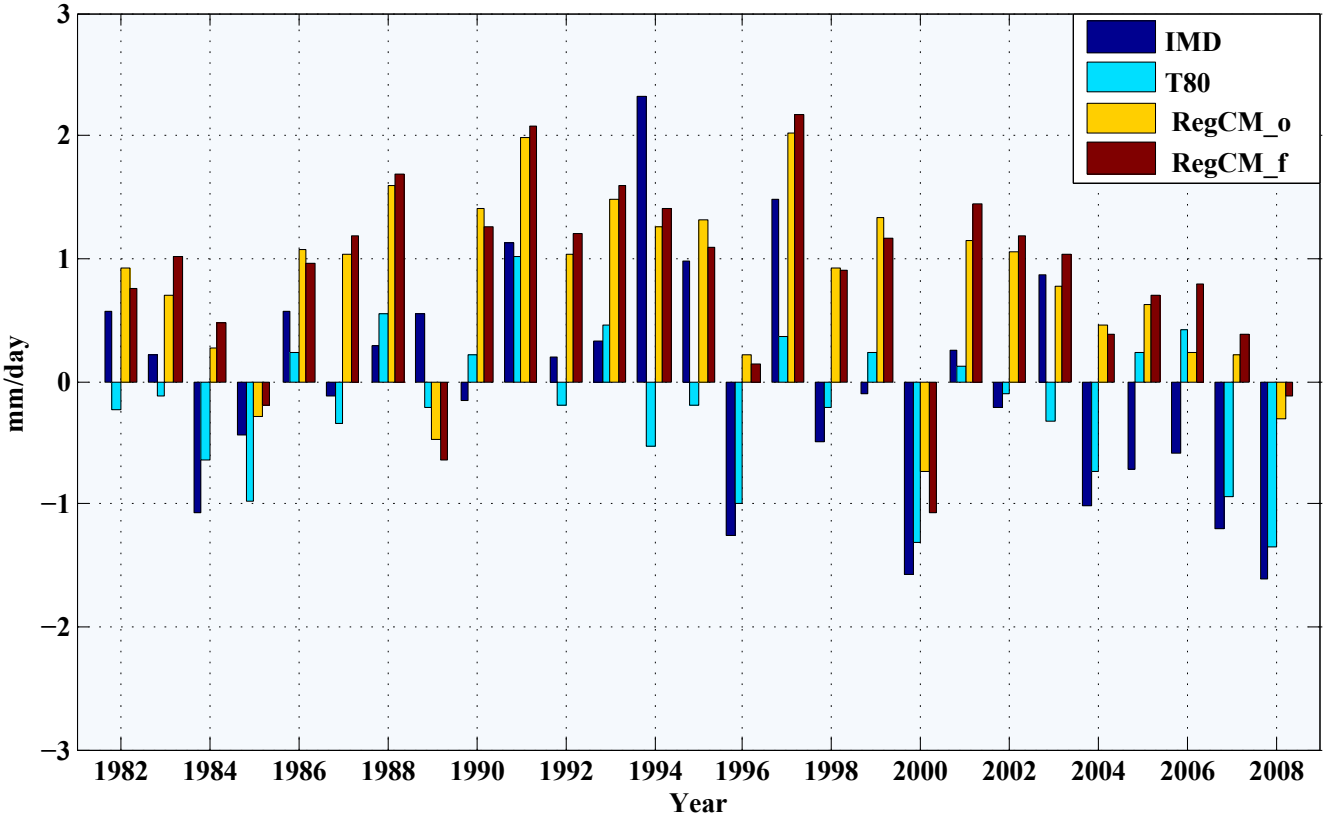

Figure 5. Precipitation anomalies (mm/day) from observation, T80 and T80 driven RegCM with observed and forecasted SST (RegCM_o and RegCM_f) for winter season over the north India region during 1982–2008.

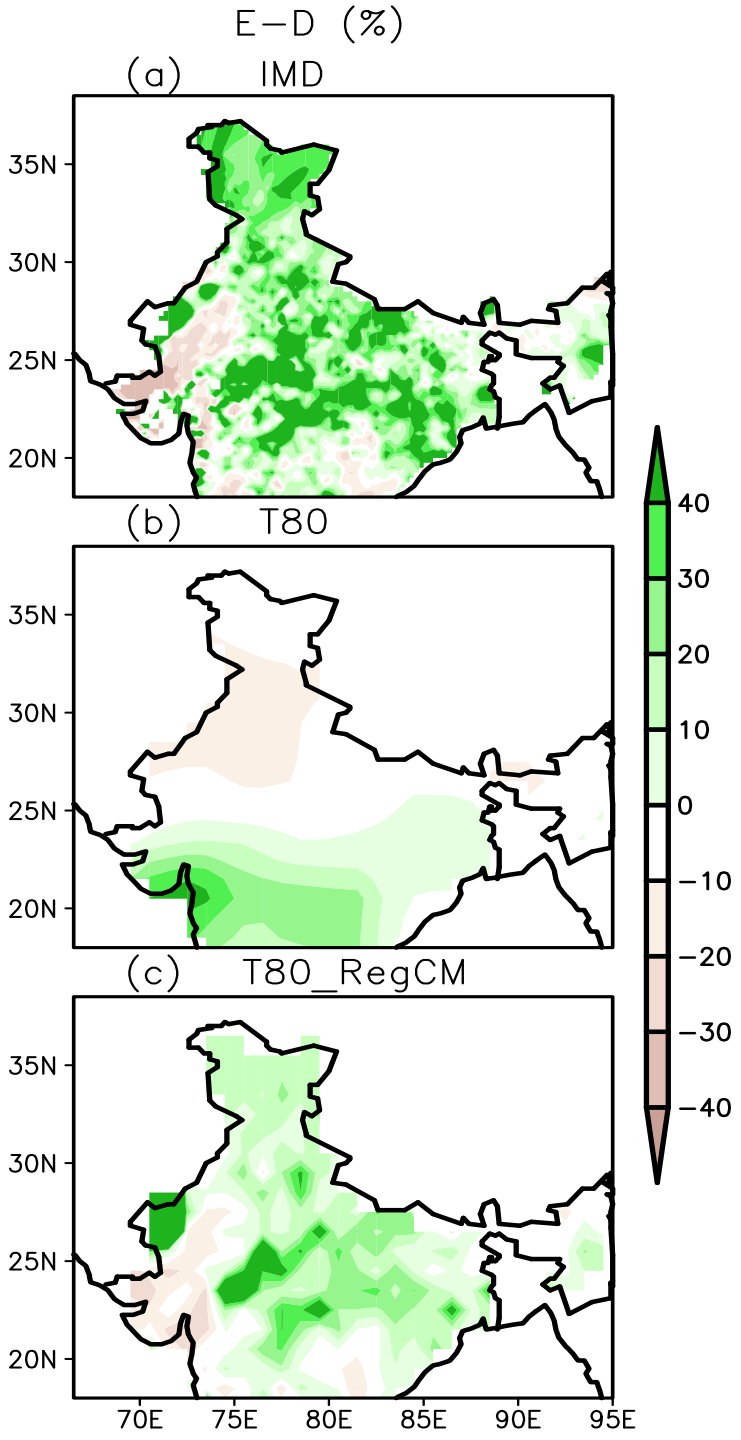

Figure 6. Percentage differences between seasonal mean (DJF) wet- and dry-year composites of precipitation from (a) observation, (b) T80 and (c) T80_RegCM model.

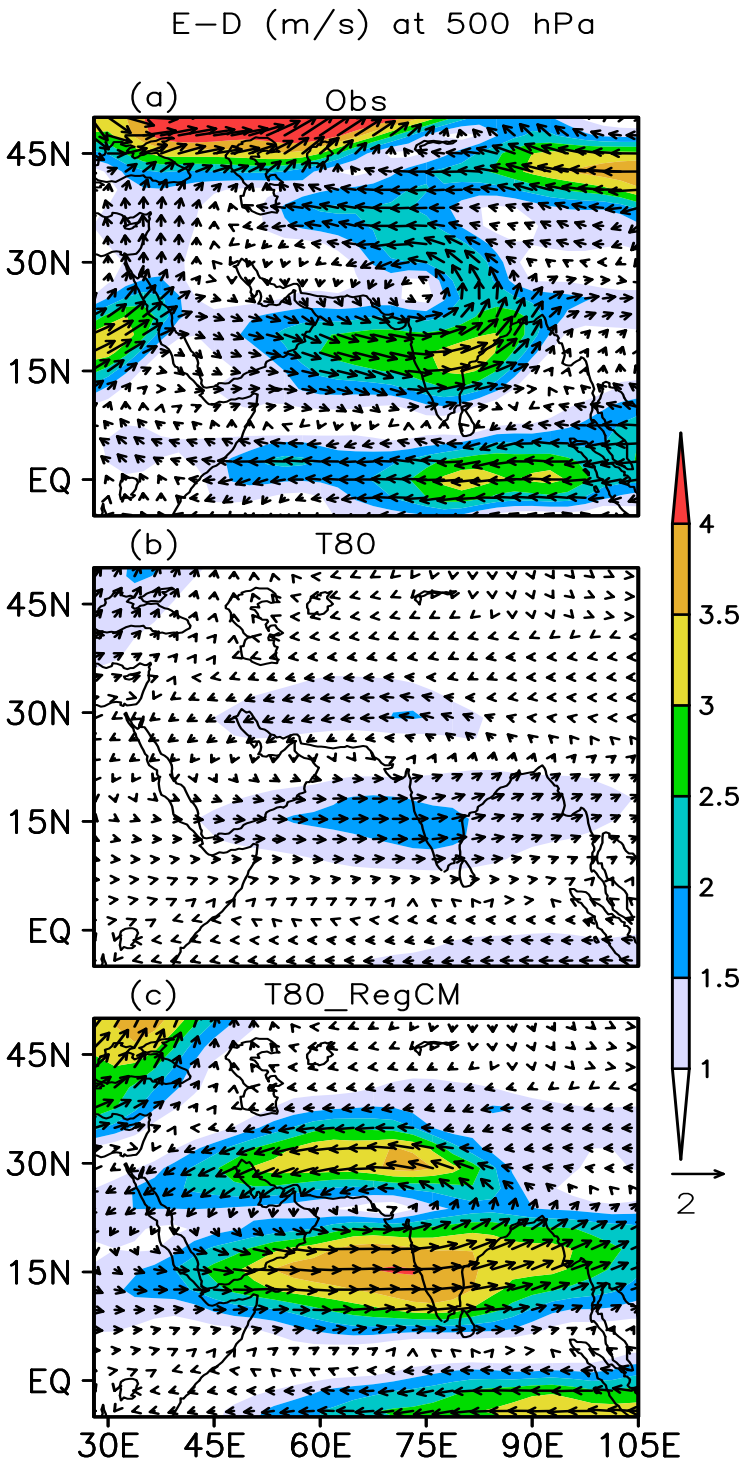

Figure 7. Differences between seasonal mean (DJF) wet- and dry-year composites of winds (in m/s) at 500 hPa from (a) observation, (b) T80 and (c) T80_RegCM model.

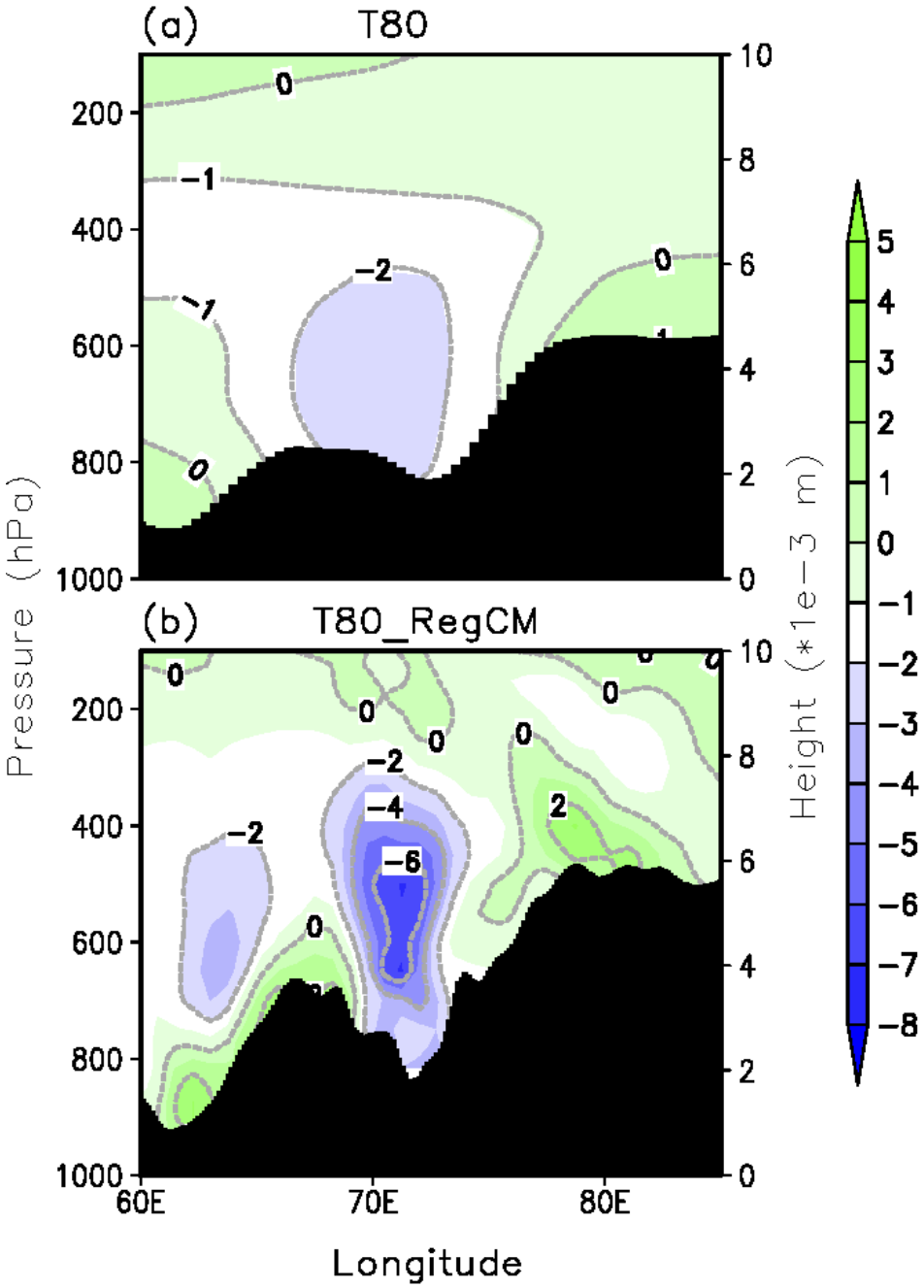

Figure 8. Longitude–height distribution of the differences between seasonal mean (DJF) wet- and dry-year composites of vertical velocity (Pa/s; shaded and broken contour) and topography (*1e-3 m; shaded bar, right-hand vertical axis) in (a) T80 and (b) RegCM at 35°N latitude.

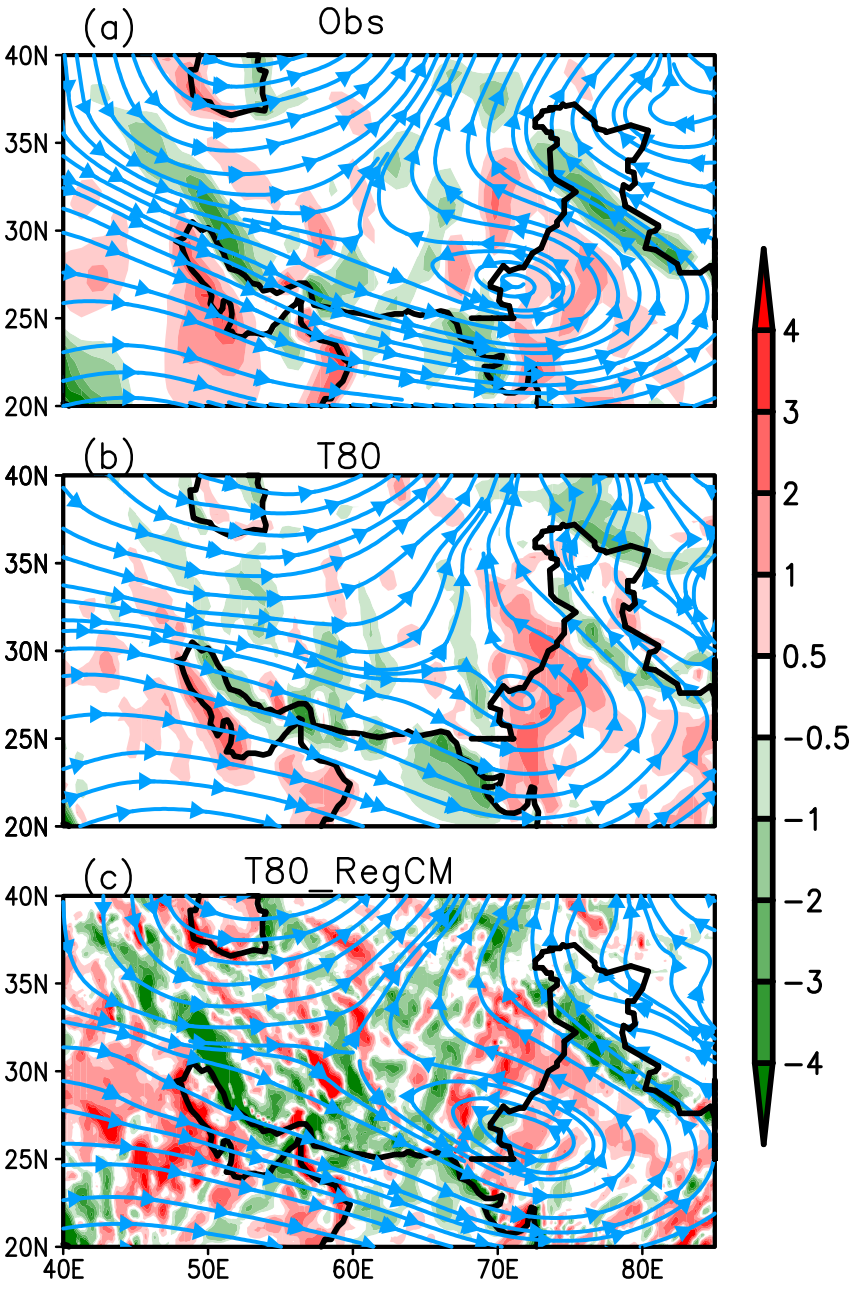

Figure 9. The difference between seasonal mean (DJF) wet- and dry-year composites of vertical integrated moisture flux (shaded) and transport (streamlines) in (a) observation, (b) T80, and (c) T80 and T80 driven RegCM (T80_RegCM) simulations, respectively.

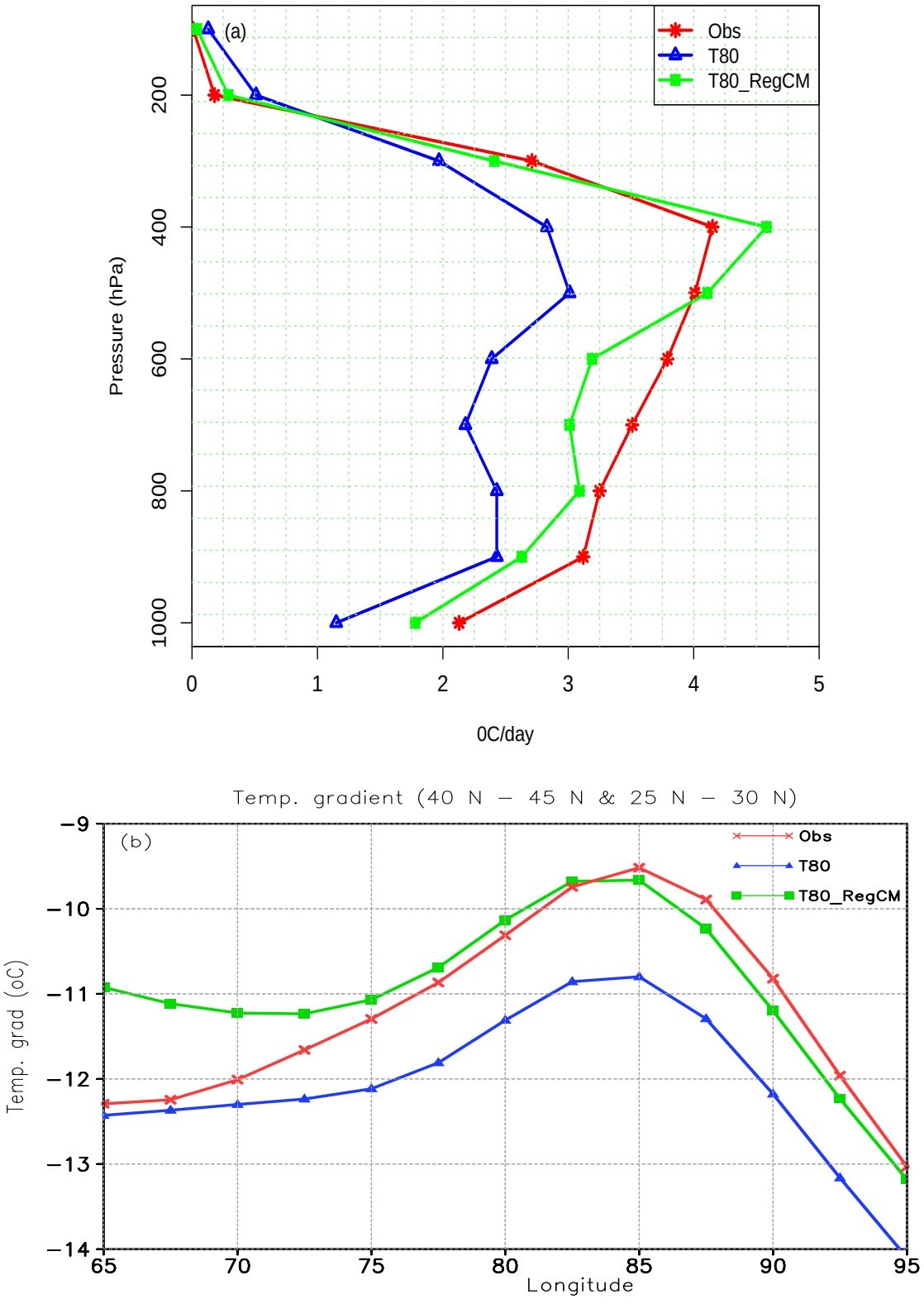

Figure 10. (a) Seasonal (DJF) mean convective heating rate (^{0}C/day) computed from NNRP2, T80 and T80 driven RegCM (T80_RegCM) models respectively; (b) Temperature gradient between two latitudinal circles (40^0 N - 45^0 N & 25^0 N – 30^0 N).

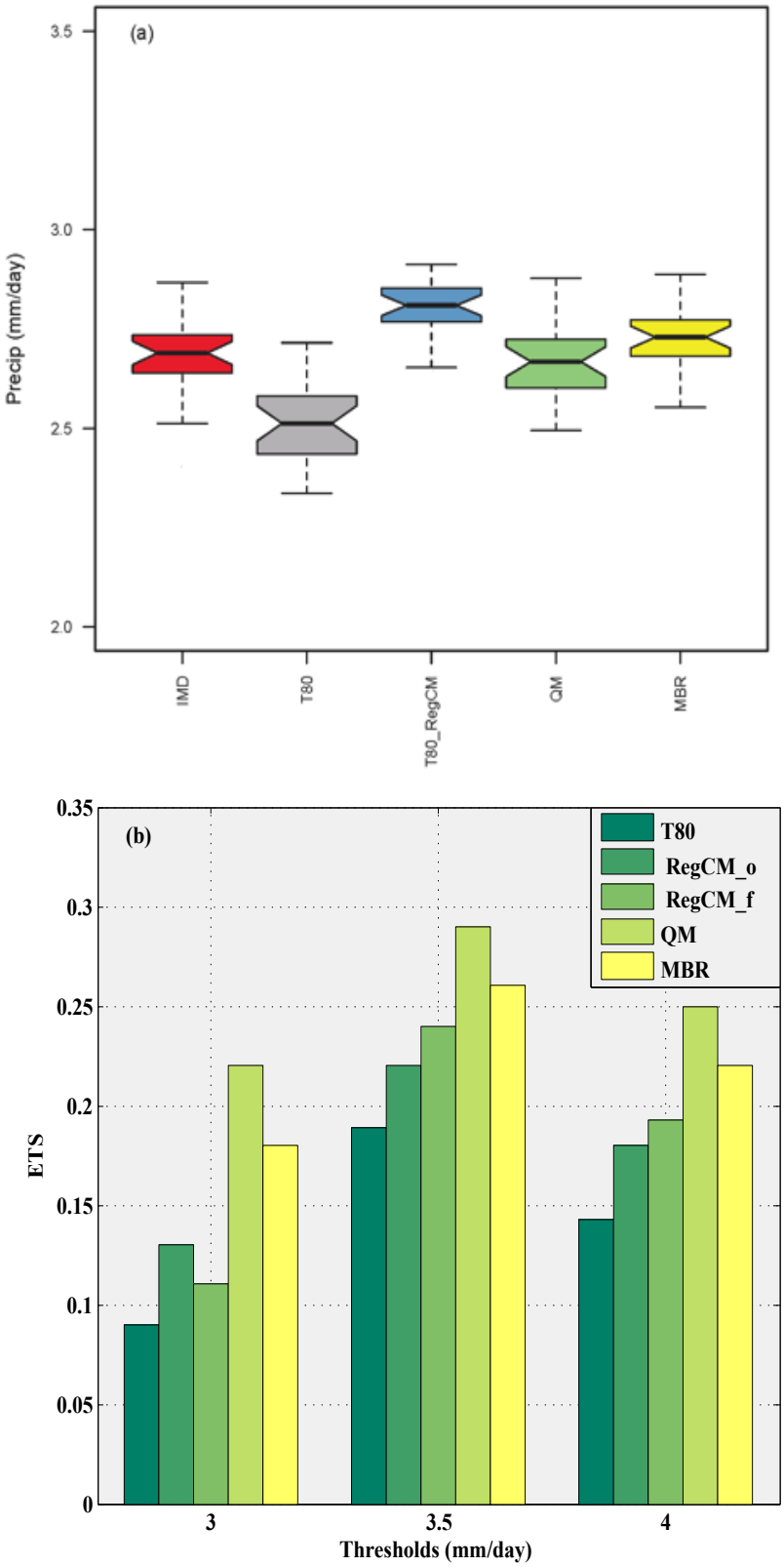

Figure 11 (a) Distribution of observed and model simulated precipitation (mm/day) for winter season. (b) Equitable threat score (ETS) computed for T80_RegCM and two bias correction methods (QM & MBR) for winter season.

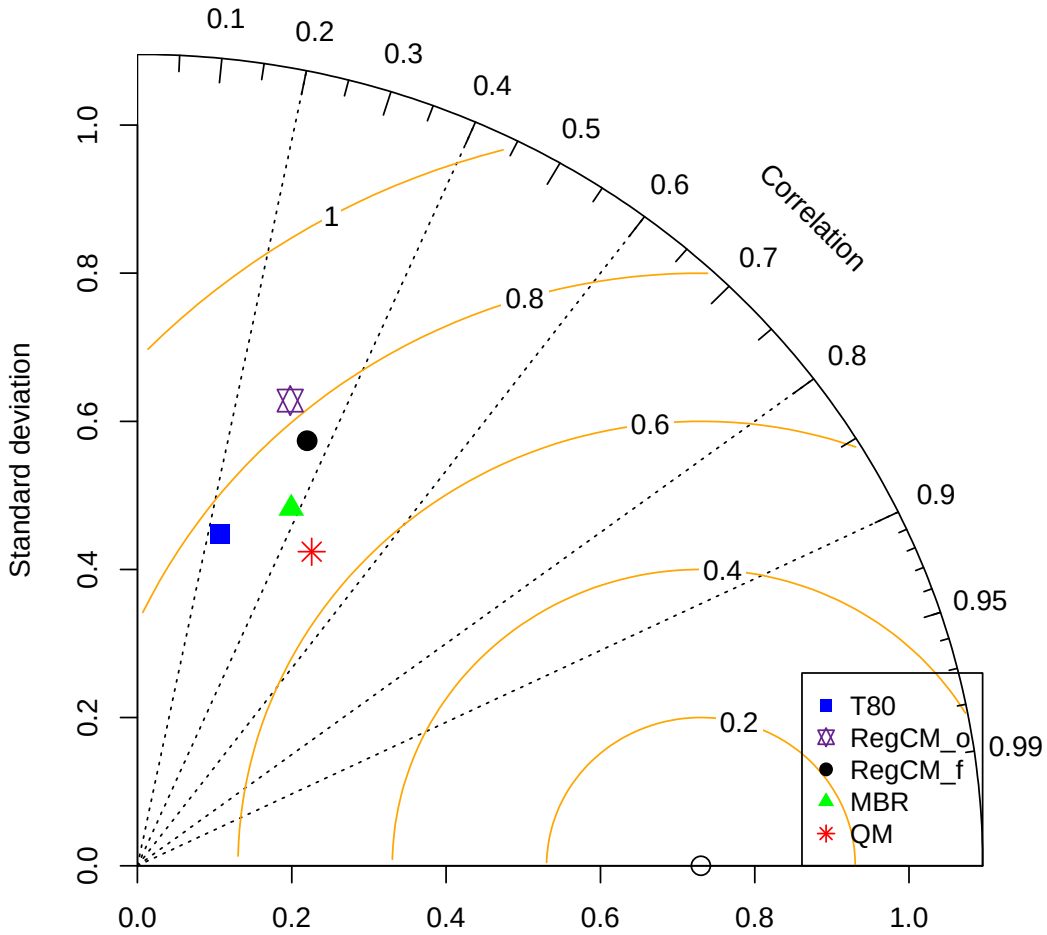

Figure 12. Taylor diagram for the north India average precipitation prediction skill of the T80, T80 driven RegCMs and two bias correction methods.

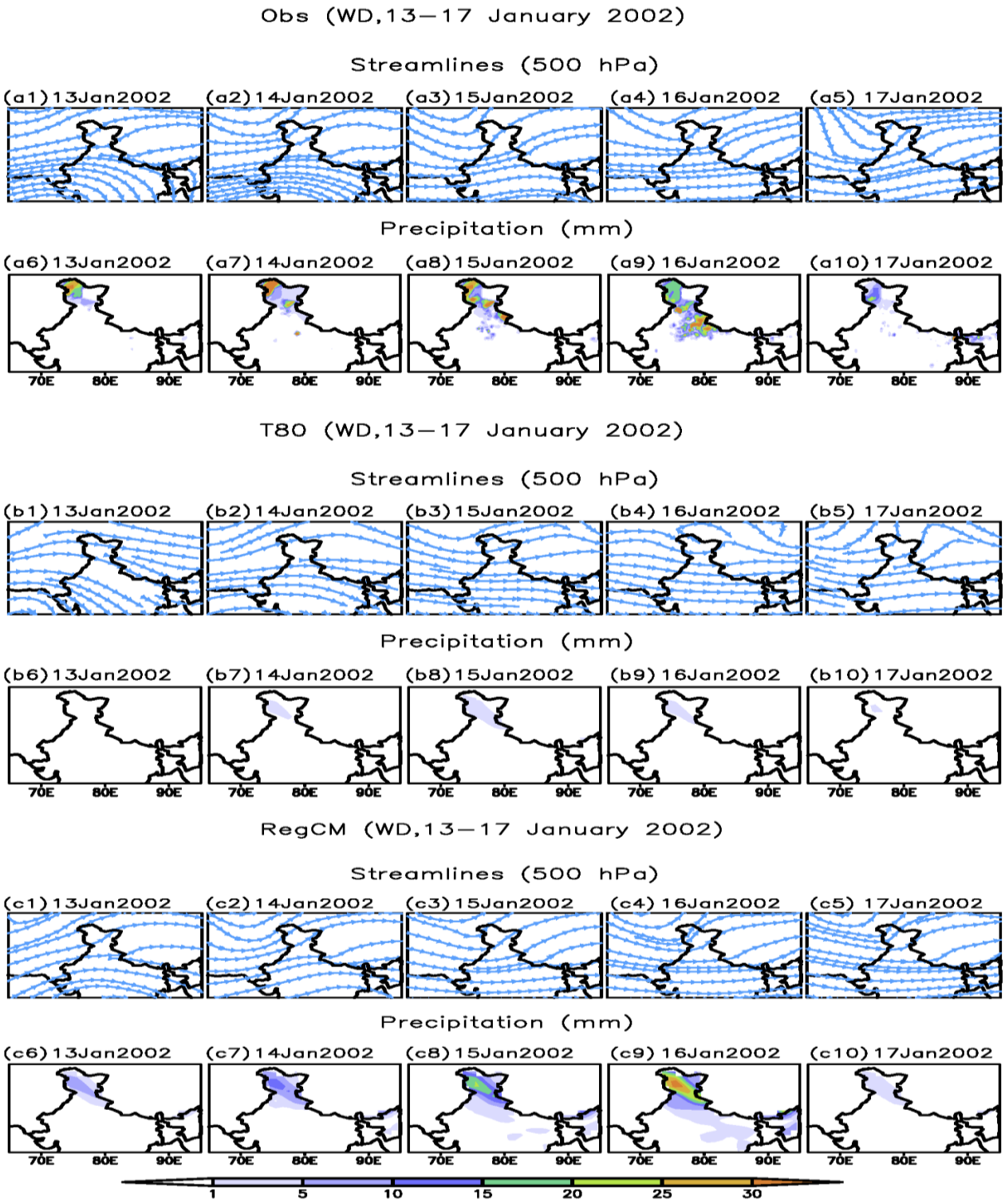

Figure 13. Observed, T80 and RegCM simulated streamline and precipitation analysis for an extreme WD case occurred during 13–17 January 2002. The upper panel shows the observed streamlines at 500 hPa (a1-a5) and precipitation (a6-a10). T80 simulated streamlines at 500 hPa (b1-b5) and precipitation (b6-b10) are shown in middle panels. The lower panels shows RegCM simulated streamlines at 500 hPa (c1-c5) and precipitation (c6-c10) respectively.

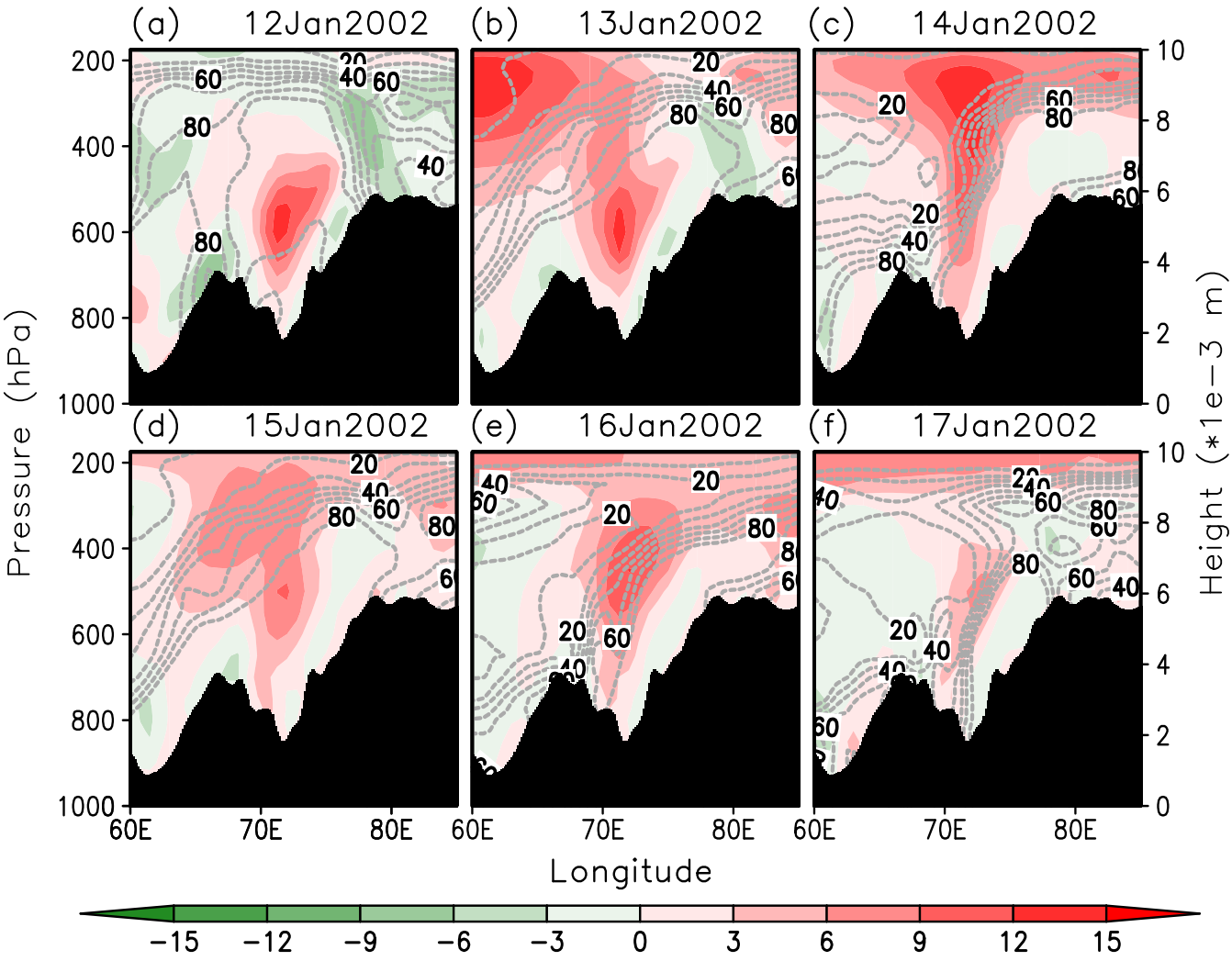

Figure 14. Longitude–height distribution of vorticity (*1e-5/s; shaded), relative humidity (%; broken contour), and topography (*1e-3 m; shaded bar, right-hand vertical axis) on (a) 12 January 2002, (b) 13 January 2002, (c) 14 January 2002, (d) 15 January 2002, (e) 16 January 2002, and (f) 17 January 2002 at 35°N latitude in the RegCM simulation.

Table 1. Configuration of RegCM4 model used in the present study

Dynamics	Hydrostatics
Main Prognostic Variables	u, v, t, q and p
Central point of domain	Latitude: 15.1^0N, longitude: 74.5^0E
Number of horizontal grid points	320 grid points along latitude and 416 grid points along longitude
Horizontal grid distance	30 km
Map projection	Lambert conformal map projection
Vertical co-ordinate	Terrain-following sigma co-ordinate
Cumulus parameterization	Grell with Fritch & Chappell closure
Land surface scheme	Community Land Model (CLM3.5)
Orography treatment	Envelop orography (10 % increase from model mean height)
Radiation parameterization	NCAR/CCM3 radiation scheme
PBL parameterization	Holtslag

Table 2. Seasonal mean precipitation over seventeen (17) stations obtained from SASE observation, T80, T80 driven RegCM (T80_RegCM) and bias corrected RegCM (BC_RCM) for composite of wet and dry years. The shaded values are closer to the observations. The model data is bi-linearly interpolated to the station locations

Station	**Composite Wet**					**Composite Dry**				
	SASE	T80	T80_RegCM	QM	MBR	SASE	T80	T80_RegCM	QM	MBR
1. Bahadur	**3.64**	3.58	4.69	3.61	3.59	**2.17**	1.79	5.02	2.24	2.21
2. Banihal	**7.81**	4.74	7.83	5.49	6.79	**3.08**	1.62	4.17	3.15	3.17
3. Bhang	**4.86**	2.42	8.69	4.90	4.91	**2.84**	2.96	5.09	3.95	4.94
4. Dhundi	**7.27**	3.26	8.87	7.31	7.29	**4.73**	3.47	4.86	4.38	4.17
5. Dras	**6.91**	4.02	9.41	7.52	7.03	**1.82**	1.73	4.13	1.68	2.43
6. Gulmarg	**7.30**	3.18	7.39	7.41	7.16	**4.13**	3.57	4.16	4.25	4.27
7. H-Taj	**7.96**	4.21	9.04	8.05	8.31	**2.34**	1.13	2.65	2.38	2.37
8.Kanzalwan	**9.85**	5.13	9.42	9.86	9.84	**3.83**	2.14	5.27	3.72	3.28
9. Kumar	**2.34**	2.29	6.39	5.14	5.78	**0.85**	1.04	3.62	3.03	1.06
10. Neeru	**5.10**	3.06	7.05	5.11	5.13	**2.79**	1.21	8.39	2.84	2.82
11. Patsio	**3.50**	2.27	4.71	3.88	3.53	**1.93**	2.32	5.15	2.46	2.11
12. Pharki	**9.03**	4.69	9.06	9.04	8.73	**4.72**	3.24	4.37	4.83	4.82
13. Solang	**8.72**	4.83	8.84	7.41	8.81	**3.38**	1.46	4.61	3.47	3.64
14. Stg-II	**10.6**	5.73	9.31	10.6	8.31	**3.74**	2.19	5.77	4.13	3.82
15. Z-Gali	**7.58**	3.09	8.97	7.59	8.43	**4.21**	3.26	4.38	4.35	4.61
16. Gugaldhar	**7.15**	2.78	7.20	7.24	7.21	**3.65**	2.92	7.66	7.67	7.78
17. Dawar	**4.63**	2.08	6.17	4.85	4.86	**2.90**	2.23	6.51	3.07	4.91